Journal Pre-proof

Pharmacological data of cannabidiol- and cannabigerol-type phytocannabinoids acting on cannabinoid CB_1, CB_2 and CB_1/CB_2 heteromer receptors

Gemma Navarro, Katia Varani, Alejandro Lillo, Fabrizio Vincenzi, Rafael Rivas-Santisteban, Iu Raïch, Irene Reyes-Resina, Carlos Ferreiro-Vera, Pier Andrea Borea, Verónica Sánchez de Medina, Xavier Nadal, Rafael Franco

PII: S1043-6618(20)31248-2

DOI: https://doi.org/10.1016/j.phrs.2020.104940

Reference: YPHRS 104940

To appear in: *Pharmacological Research*

Received Date: 19 April 2020

Revised Date: 13 May 2020

Accepted Date: 15 May 2020

Please cite this article as: { doi: https://doi.org/

Title:

Pharmacological data of cannabidiol- and cannabigerol-type phytocannabinoids acting on cannabinoid CB_1, CB_2 and CB_1/CB_2 heteromer receptors.

Authors

Gemma Navarro[1,2], Katia Varani[3], Alejandro Lillo[1,4], Fabrizio Vincenzi[3], Rafael Rivas-Santisteban[2,4], Iu Raïch[2,4], Irene Reyes-Resina[2,4,#], Carlos Ferreiro-Vera[5], Pier Andrea Borea[6], Verónica Sánchez de Medina[5], Xavier Nadal[7], Rafael Franco[2,4]

Affiliations

1. **Department of Biochemistry and Physiology. School of Pharmacy and Food Sciences. Universitat de Barcelona, Spain.**
2. **Centro de Investigación Biomédica en Red sobre Enfermedades Neurodegenerativas (CiberNed), Spain.**
3. **Department of Morphology, Surgery and Experimental Medicine, Ferrara University, Ferrara, Italy.**
4. **Department of Biochemistry and Molecular Biomedicine. Universitat de Barcelona, Spain.**
5. **Phytoplant Research S.L., Córdoba, Spain.**
6. **Ferrara University, Ferrara, Italy.**
7. **Independent Researcher, Córdoba, Spain.**

 # Current address: Research Group: Neuroplasticity, Leibniz Institute for Neurobiology, 39118, Magdeburg, Saxony-Anhalt, Germany.

Corresponding author

Rafael Franco
Centro de Investigación Biomédica en Red sobre Enfermedades Neurodegenerativas (CiberNed). Valderrebollo, 5. 28031 Madrid. Spain
Tel. +34 934021208
rfranco@ub.edu; rfranco123@gmail.com

Running title

Biased signaling disclosed by phytocannabinoids

Graphical Abstract

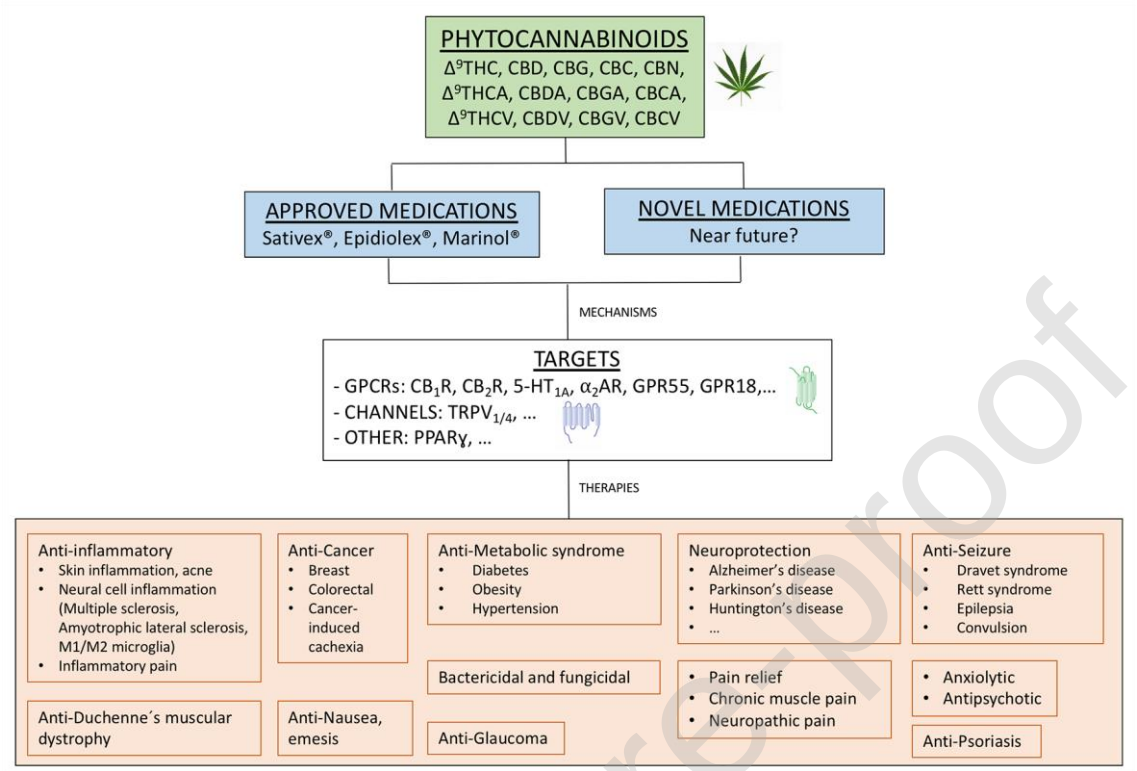

Abstract

Background: Recent approved medicines whose active principles are Δ^9Tetrahidrocannabinol (Δ^9-THC) and/or cannabidiol (CBD) open novel perspectives for other phytocannabinoids also present in *Cannabis sativa* L. varieties. Furthermore, solid data on the potential benefits of acidic and varinic phytocannabinoids in a variety of diseases are already available. Mode of action of cannabigerol (CBG), cannabidiolic acid (CBDA), cannabigerolic acid (CBGA), cannabidivarin (CBDV) and cannabigerivarin (CBGV) is, to the very least, partial.

Hypothesis/Purpose: Cannabinoid CB_1 or CB_2 receptors, which belong to the G-protein-coupled receptor (GPCR) family, are important mediators of the action of those cannabinoids. Pure CBG, CBDA, CBGA, CBDV and CBGV from *Cannabis sativa* L. are differentially acting on CB_1 or CB_2 cannabinoid receptors.

Study Design: Determination of the affinity of phytocannabinoids for cannabinoid receptors and functional assessment of effects promoted by these compounds when interacting with cannabinoid receptors.

Methods: A heterologous system expressing the human versions of CB_1 and/or CB_2 receptors was used. Binding to membranes was measured using radioligands and binding to living cells using a homogenous time resolved fluorescence resonance energy transfer (HTRF) assay. Four different functional outputs were assayed: determination of cAMP levels and of extracellular-signal-related-kinase phosphorylation, label-free dynamic mass redistribution (DMR) and ß-arrestin recruitment.

Results: Affinity of cannabinoids depend on the ligand of reference and may be different in membranes and in living cells. All tested phytocannabinoids have agonist-like behavior but behaved as inverse-agonists in the presence of selective receptor agonists. CBGV displayed enhanced potency in many of the functional outputs. However the most interesting result was a biased signaling that correlated with differential affinity, i.e. the overall results suggest that the binding mode of each ligand leads to specific receptor conformations underlying biased signaling outputs.

Conclusion: Results here reported and the recent elucidation of the three-dimensional structure of CB_1 and CB_2 receptors help understanding the mechanism of action that might be protective and the molecular drug-receptor interactions underlying biased signaling.

List of Abbreviations

Δ^9-THC: Δ^9Tetrahidrocannabinol
5-HT_{2A} receptor: serotonin$_{2A}$ receptor
BRET: Bioluminescence Resonance Energy Transfer
cAMP: cyclic adenosine monophosphate
CB_1R: cannabinoid receptor 1
CB_2R: cannabinoid receptor 2
$CB_{1/2}$RHets: CB_1R- CB_2R heteroreceptor complexes
CBD: cannabidiol
CBDA: cannabidiolic acid
CBDV: cannabidivarin
CBG: cannabigerol
CBGA: cannabigerolic acid
CBGV: cannabigerivarin
CHO: Chinese Hamster Ovary
D_1R dopamine receptor 1
DMEM: Dulbecco's Modified Eagle Medium
DMR: dynamic mass redistribution
ERK: extracellular signal-regulated kinases
GFP^2: green fluorescent protein 2
GPCRs: G-protein-coupled receptors
GTP: guanosine 5 triphosphate
HEK: Human Embryonic Kidney
HTRF: Homogeneous time-resolved fluorescence resonance energy transfer
IC_{50}: half maximal inhibitory concentration

K_D: dissociation constant
K_i: inhibition constant
MAPK: mitogen-activated protein kinase
PBS: phosphate-buffered saline
PKA: protein kinase A
RLuc: *Renilla luciferase*
TLB: Tag-lite buffer
YFP: yellow fluorescent protein

Keywords

Cytocrin, phytocannabinoids, biased signaling, homogeneous binding, radioligand binding, GPCR structure

Introduction

Cannabis is the most widely used illicit substance although, recently, cannabis-derived substances have been approved for medicinal purposes. Plant-derived cannabinoids show from a characteristic psychoactive effect, which can lead to either serious neurological and/or neuropsychiatric problems, to beneficial effects in, among other, chronic pain, diabetes, obesity, anorexia and neurodegenerative diseases [1–5].
(6aR,10aR)-6,6,9-Trimethyl-3-pentyl-6a,7,8,10a-tetrahydro-6H-benzo[c]chromen-1-ol (CAS#1972-08-3) or Δ^9Tetrahidrocannabinol (Δ^9-THC) and 2-[(1R,6R)-6-Isopropenyl-3-methyl-2-cyclohexen-1-yl]-5-pentyl-1,3-benzenediol (CAS#13956-29-1) or cannabidiol (CBD) are the most recognized and studied phytocannabinoids. In the form of plant extracts or in galenic preparations, medicines containing CBD, Δ^9-THC or the two compounds (Epidiolex™, Marinol™, Sativex™) have been approved by regulatory bodies and can be used in humans affected of very specific diseases. *Cannabis sativa* L. plant and Cannabis, as a drug, contain other compounds that have structural similarities with Δ^9-THC and CBD. Some of the common *Cannabis sativa* L. varieties are enriched in these compounds that have been extensively studied from a chemical, biological, physiological and pharmacological perspective. However, there are other varieties that are enriched in other molecules and, overall, more than 400 compounds can be isolated from a single plant of which circa 150 are considered, in the basis of the chemical structure, phytocannabinoids [6]. Currently, the focus is on the minor, varinic, acidic and minority phytocannabinoids, among other cannabigerol (CBG), cannabidiolic acid (CBDA), cannabigerolic acid (CBGA), cannabidivarin (CBDV) and cannabigerivarin (CBGV). As a matter of fact, CBG-enriched varieties were already described in 1987 [7].

At first, it was assumed that the effects of all phytocannabinoids were mediated by CB_1 (CB_1R) and CB_2 (CB_2R) receptors, which belong to the superfamily of G-protein-coupled receptors (GPCRs). Doubts arose when reported physiological actions for some of those compounds occur at concentrations that are unable to significantly affect (agonistically or antagonistically) these receptors. It should be noted that GPCRs may form dimers or supramolecular complexes with properties that are different from those of individual receptors. Relevant for this paper is the physiologically-relevant interaction discovered for the two cannabinoid receptors that are able to form heteromers ($CB_{1/2}RHets$) [8,9]. Other possible targets that have already been described are vanilloid cell surface channels and peroxisome proliferator-activated receptor gamma (PPARγ) [10–12]. Orphan GPCRs that share homology with cannabinoid receptors and/or are in vitro modulated by cannabinoids are also potential targets of phytocannabinoids; two relevant examples are GPR55 and GPR18 [13–18]. A nice account of the complex scenario due to both the variety of potential targets of phytocannabinoids and the fact that a given compound may act in different targets is provided in [19].

If compared with other GPCRs of the same family (class A rhodopsin-like), the structure of cannabinoid receptors has differential traits that explain why they are activated by compounds having an important hydrophobic character [20–23]. For instance, in the case of the CB_2 receptor, the orthosteric center is somewhat hidden and the agonists may cross a vestibule located at the level of the lipid bilayer to get inside the orthosteric center. Furthermore, CBD has been described as an allosteric modulator of both CB_1 and CB_2 receptors [24,25]. Besides, GPCRs display functional selectivity leading to biased signaling, i.e. different compounds may lead to different outputs via the same receptor [26–28].

There are already numerous reports suggesting benefits of phytocannabinoids other than CBD and Δ^9-THC. At present, CBGA, CBGV, CBDA and/or CBDV are considered as promising to combat a huge variety of diseases. A review of the therapeutic potential of varinic and acidic phytocannabinoids has been recently released [29]. For instance, CBG is considered as antimicrobial [30,31] and as counteracting neuroinflammation targeting glial cells [32]. Potential to combat for amyotrophic lateral sclerosis is based in the actions of a synthetic derivative, VCE-003.2, in the SOD1G93A rodent model of the disease [33,34]. CBG seems to inhibit ALR2 aldose reductase, which is of relevance in diabetes [35], and to be of interest in eating disorders as it produces both hyperphagia in rats [36] and leads to further food consumption in satiated rats [37]. In addition, CBG is proposed to combat skin diseases such as dryness, acne or psoriasis [38–40]. Finally, CBG has been proposed to combat Parkinson's and Huntington's diseases (see [41] for review), some types of cancer [42] and inflammatory bowel disease [43,44]. Despite the cumulative information about the therapeutic potential, the effect of CBG on cannabinoid receptors is partially known; CBG seems to be agonist of one receptor and antagonists of the other [32,45,46]. In the case of varinic and acidic compounds the information is fairly poor; either there is no information on compounds targeting cannabinoid receptors or it is controversial. Accordingly, the aim of this paper was to undertake binding and signaling assays to characterize the pharmacology

of varinic and acidic phytocannabinoids on cannabinoid receptors also focusing on trends that could help understanding biased signaling via CB_1R, CB_2R and $CB_{1/2}RHets$.

To decipher the pharmacology of CBGA, CBGV, CBDA and CBDV on CB_1R, CB_2R and $CB_{1/2}RHets$, binding assays were performed using two different techniques and three unrelated chemical compounds. We also analyzed whether phytocannabinoids were able to modulate receptor expression and we also investigated the functional effect and the bias towards different signaling pathways. Chemical structures for CBG, CBGA, CBGV, CBD, CBDA and CBDV are shown in Supplementary Fig. S1.

Results

BRET reflecting direct CB_1-CB_2 receptor interactions is enhanced by CBDA but not by CBD, CBG, CBGA, CBGV or Δ^9-THC.

It has been demonstrated that cannabinoid receptors CB_1 and CB_2 can interact to form $CB_{1/2}RHets$ complexes [8,9]. In these complexes the CB_2R blocks CB_1R-mediated induced effects. Then, we questioned if cannabinoid compounds could alter CB_1-CB_2 receptor complex ($CB_{1/2}RHet$) formation. HEK-293T cells were transfected with a constant amount of cDNA for CB_1R-RLuc and increasing amounts of cDNA for CB_2R-GFP^2 and a saturable BRET curve ($BRET_{max}$ 214±15, $BRET_{50}$ 48±9) indicated a specific interaction of CB_1R with CB_2R (Fig. 1A). However, when HEK-293T cells were transfected with cDNA for CB_1R-RLuc and increasing amounts of cDNA for D_1R-GFP^2, the linear signal indicated a lack of interaction. Conditions to provide a signal close to $BRET_{max}$ were selected to analyze the effect of cannabinoid compounds. Then, HEK-293T cells were transfected with a constant amount of cDNA for CB_1R-RLuc and CB_2R-GFP^2 and treated with 100 nM CBG, CBGA, CBGV, CBD, CBDA or CBDV. Interestingly, it was observed that CBD treatment induced a significant decrease in BRET signal (Fig. 1B). These results indicate that CBD treatment could decrease the formation of complexes or induce a readjustment in CB_1R-CB_2R complex structure that separates RLuc from GFP^2. In contrast, CBDA markedly increased CB_1R-CB_2R complex formation and/or induced structural changes, that led to a decrease in the distance between RLuc and GFP^2 proteins (Fig. 1B). The other compounds did not significantly affect BRET values.

Figure 1

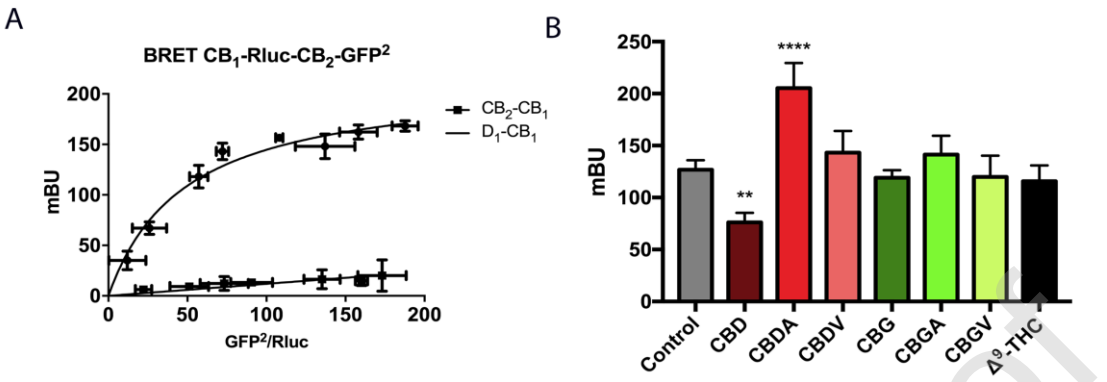

Figure 1. Cannabinoid receptor expression in cells treated with CBDA, CBDV, CBGA and CBGV. Panel A: BRET in HEK-293T cells transfected with a constant amount of cDNA for CB_1R-RLuc (0.7 μg) and increasing amounts of cDNA for CB_2R-GFP^2 (0.2-1 μg) or D_1R-GFP^2. Panel B: $BRET_{max}$ measured in HEK-293T cells transfected with 0.7 μg cDNA for CB_1R-RLuc and 0.6 μg cDNA for CB_2R-GFP^2 and treated with 100 nM of CBD, CBDA, CBDV, CBG, CBGA, CBGV, Δ^9-THC or vehicle 10 min before coelenterazine H addition. Data are the mean ± SEM (n=6 performed in triplicates). One-way ANOVA and Bonferroni's multiple comparison *post-hoc* tests were used for statistics analysis (**p<0.01 and ***p<0.001 versus control).

CBDA affinity is in the micromolar range in radioligand-based assays using either CB_1R- or CB_2R-containing membranes.

To analyze affinity at both cannabinoid CB_1 and CB_2 receptors, radioligand binding competition assays were performed using [^{3}H]-CP-55940 and increasing concentrations of compounds (from 10 nM to 30 μM) in membranes isolated from CHO cells expressing human CB_1 or CB_2 receptors. K_i values for CBDA obtained using [^{3}H]-CP-55940 as radioligand were in the low micromolar range for both CB_1R (K_i = 626 ± 52 nM) and CB_2R (K_i = 813 ± 62 nM) (Fig. 2B). Interestingly, competition curves obtained using CB_1R- or CB_2R-containing membranes were superimposable. K_i values were similar for CBG (K_i CB_1R = 1,045 ± 74 nM; K_i CB_2R = 1,225 ± 85 nM) and CBD (K_i CB_1R = 1,690 ± 110 nM; K_i CB_2R = 1,714 ± 70 nM). In contrast, CBGA (K_i CB_1R = 13,116 ± 1,047nM; K_i CB_2R = 17,348 ± 987 nM) had lower affinity than CBG and CBGV (K_i CB_1R = 2,865 ± 160 nM; K_i CB_2R = 3,005 ± 127 nM) at both cannabinoid receptors. Furthermore, CBGA at the highest concentration used was not able to completely displace [^{3}H]-CP-55940 binding. Also interestingly, the varinic CBGV compound had higher affinity than the varinic CBDV (K_i CB_1R = 14,445 ± 999 nM; K_i CB_2R = 15,719 ± 975 nM) compound, which at the highest concentration used was unable to completely displace [^{3}H]-CP-55940 binding. In summary, in competition assays, i) CBDA was the molecule with higher affinity closely followed by

CBG and CBD, ii) CBDA was more efficacious than CBGA and iii) CBGV was more efficacious that CBDV (Fig. 2). In fact, both CBGA and CBDV displayed a fairly low affinity (Table 1).

Similar experiments were undertaken using [^{3}H]-WIN-55,212-2 and the results showed both similarities and differences respect to those encountered using [^{3}H]-CP-55940. Remarkably, although the qualitative behavior was different on CB_1R or on CB_2R-containing membranes, CBDA, CBG, CBD and CBGV led to similar quantitative results. On the one hand, CBDA, CBG, CBD and CBGV were able to compete radioligand binding to CB_2R but not to CB_1R. K_i values for competing binding to the CB_2R were similar: for CBDA (K_i = 2,434 ± 142 nM), CBG (K_i = 2,656 ± 130 nM), CBD (K_i = 4,019 ± 342 nM) and CBGV (K_i = 8,089 ± 769 nM). On the other hand, CBGA did not compete for the binding to any of the receptors and CBDV did not compete for the binding to the CB_1R and very mildly for the binding to CB_2R (Supplementary Fig. S2).

In summary, CBDA displayed the highest affinity for both cannabinoid receptors with K_i values in the low micromolar range when competing with [^{3}H]-CP-55940 or [^{3}H]-WIN-55,212-2 bindings. Surprisingly, only significant competition in the binding to the CB_1R was observed when using [^{3}H]-CP-55940 as radioligand.

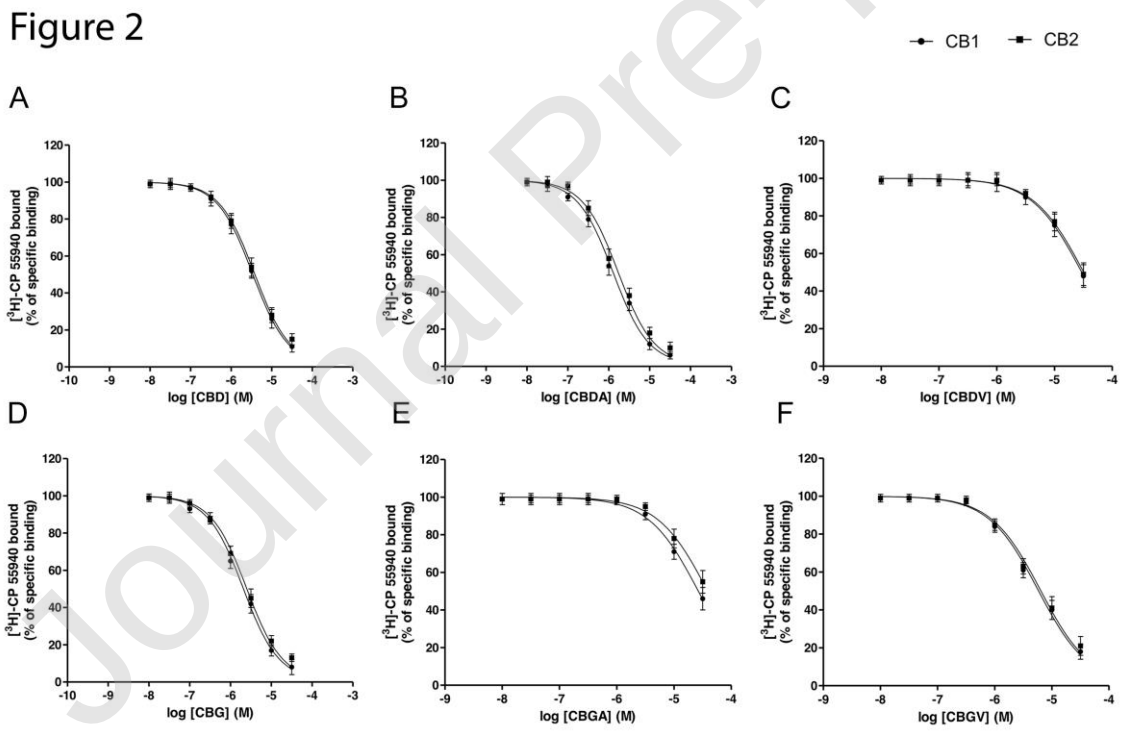

Figure 2. Competition binding experiments of [^{3}H]-CP 55940 binding to membranes isolated from CHO cells expressing CB_1R or CB_2R. Panels A-F: Competition binding experiments were developed with the specific binding of 2 nM

[^{3}H]-CP 55940 and increasing concentrations of CBD (A), CBDA (B), CBDV (C), CBG (D), CBGA (E) or CBGV (F) (0-30 μM). Data are expressed as the mean ± SEM (n=5 in duplicates).

HTRF competition binding experiments in cells expressing $CB_{1/2}$RHets

While there are no tools to perform homogeneous binding assays in the case of the CB_1R, the fluorophore-conjugated CM157 compound allow determining affinities in homogeneous assays performed in living cells in the absence of any radioligand (details in [47]). Competition assays were performed in living HEK-293T cells expressing Lumi4-Tb-labeled SNAP-CB_2R incubated with a fixed amount of the fluorophore-conjugated selective CB_2R agonist (CM157) and increasing concentrations of cannabinoids (from 0.1 nM to 10 μM). All compounds decreased the binding of labeled CM157 to SNAP-CB_2R in monophasic fashion (Fig. 3). CBD, CBDA, CBG and CBGV showed IC_{50} values in the high nanomolar range (order of affinities: CBGV ≈ CBG > CBD ≈ CBDA), whereas those of CBDV and CBGA were in the 1-10 μM range (order of affinities: CBGA > CBDV) (Table 2). Finally, we repeated the experiments in cells coexpressing the two receptors in order to detect whether the CB_1R affects the binding of cannabinoids to the CB_2R. In all cases the binding was very similar with the exception of CBDA, whose binding to the CB_2R was markedly decreased (≈ one order-of-magnitude less affinity) (Table 2).

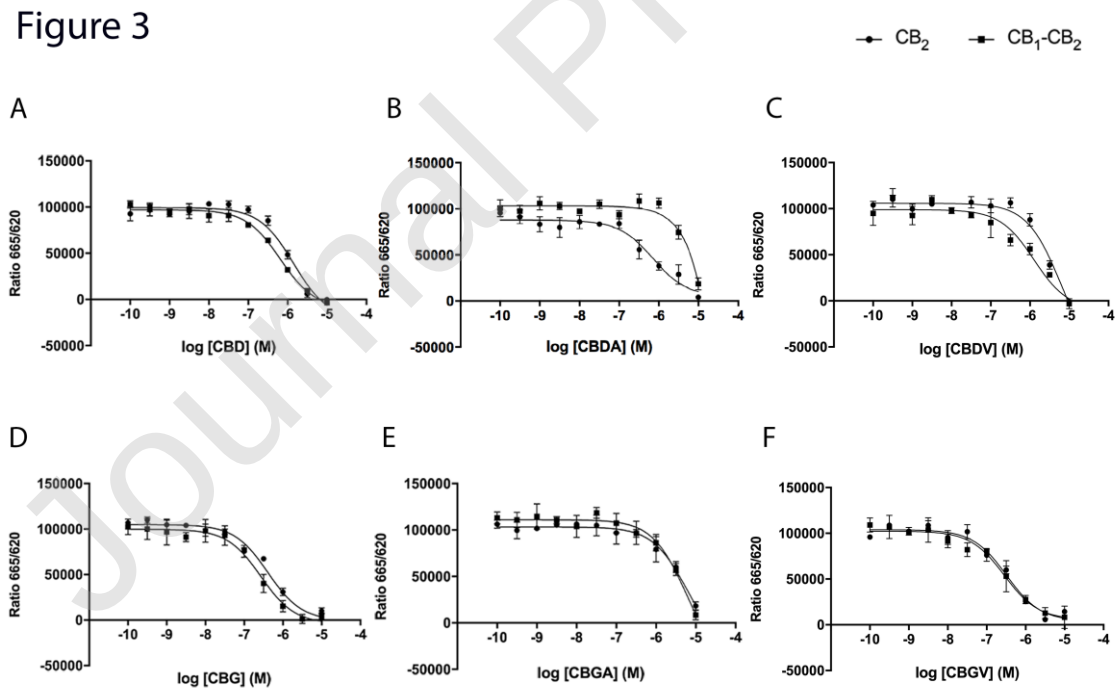

Figure 3. Competition binding experiments of CM157 red ligand to living HEK-293T cells expressing CB_2R or $CB_{1/2}$RHets. Panels A-F: Competition binding

experiments were performed in HEK-293T cells transfected with 1 μg cDNA for SNAP-CB_2R in the presence (red line) or in the absence (black line) of 0.5 μg cDNA for CB_1R. Tb labeling was performed as described in Methods. Competition binding curves were obtained by HTRF using 20 nM of red CM157 and increasing concentrations of CBD (A), CBDA (B), CBDV (C), CBG (D), CBGA (E) or CBGV (F) (0-10 μM). Data represent the mean ± SEM (n = 6 in triplicates). HTRF ratio = 665 nm acceptor signal/620 nm donor signal x 10,000.

In summary, competition data in homogeneous binding to the CB_2R in living cells is similar to that found using either [^{3}H]-CP-55940 or [^{3}H]-WIN-55,212-2, with the exception of CBDA binding that became negligible when the CB_1R was also expressed. That effect can be explained by the structural changes that occur in each cannabinoid receptor upon the formation of the $CB_{1/2}$RHets, that make more difficult for the CBDA to reach the orthosteric pocket of the CB_2R and displace the fluorophore-conjugated CM157.

Signaling assays

HEK-293T cells expressing CB_1R were treated with increasing concentrations (from 0.1 nM to 10 μM) of CBD, CBDA, CBDV, CBG, CBGA, CBGV and, as a control, Δ^9-THC. The decrease in cytosolic cAMP levels previously increased by forskolin treatment (see Methods) showed that i) CBGA and CBGV were more potent than Δ^9-THC and CBG and ii) CBDV and CBDA were as potent as Δ^9-THC and more potent than CBD. In CB_1R-expressing cells all compounds, besides CBD and CBG, acted as full agonists, with CBGA and CBGV having more potency than Δ^9-THC in decreasing the cytosolic cAMP levels previously increased by forskolin treatment. As previously described [48], the reference phytocannabinoid Δ^9-THC had negligible effect in CB_2R-containing cells. In CB_2R-expressing cells only CBDA, CBDV and CBGV acted as full agonists. In $CB_{1/2}$RHet-expressing cells compounds displayed similar potency and maximal effect, which was lower than the maximal effect found in cells only expressing CB_1 or CB_2 receptors (Fig. 4A,E,I).

Figure 4

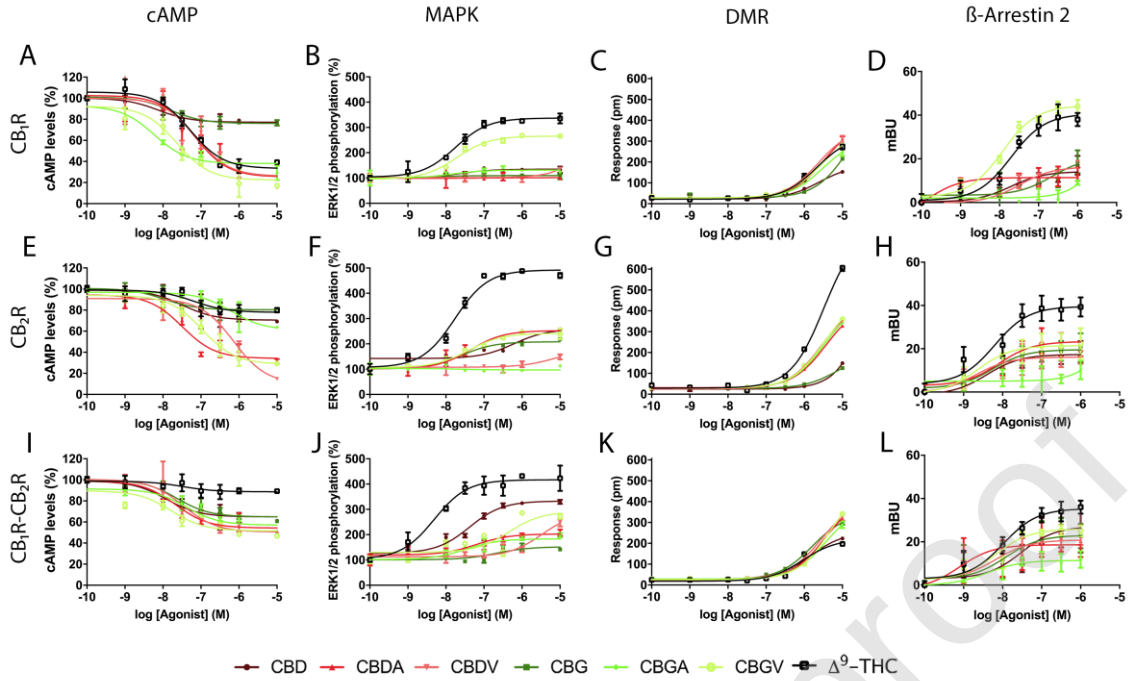

Figure 4. Signaling assays in cells expressing CB_1R, CB_2R or $CB_{1/2}RHets$. HEK-293T cells were transfected with cDNAs encoding for CB_1R (0.75 μg cDNA) (A-C), CB_2R (1 μg cDNA) (E-G) or CB_1R (0.75 μg cDNA) and CB_2R (1 μg cDNA) (I-K). In panels D, H and L β-arrestin-RLuc (1 μg cDNA) was also expressed. In each case cells were treated with CBD, CBDA, CBDV, CBG, CBGA, CBGV, Δ^9-THC or vehicle. Data in dose–response curves for reduction of forskolin-induced cAMP production (0.1 nM to 10 μM range) are expressed in % respect to the effect of forskolin (0.5 μM, 100 %) (A, E, I). Dose-response curves for ERK1/2 phosphorylation (B, F, J) and β-arrestin recruitment (D, H, L) (0.1 nM to 10 μM range) were analyzed and data are expressed as increases in % over basal. Data represent the mean ± SEM (n = 6 in triplicates). Data in dose–response curves for DMR (C, G, K) are expressed as maximum response at the indicated concentrations (0.1 nM to 1 μM range); data from a representative experiment is shown.

When MAPK pathway activation was analyzed, the results shown in Fig. 4B,F,J were markedly different to those obtained in cAMP determination assays. In CB_1R-expressing cells only the reference phytocannabinoid Δ^9-THC and CBGV were able to produce a 5 times fold increase of ERK phosphorylation. CBG and CBGA were able to increase ERK phosphorylation with a decreased potency. In CB_2R-expressing cells, CBD, CBDA, CBG and CBGV were able to increase by 2-fold ERK1/2 phosphorylation but only reaching half of the maximal effect due to Δ^9-THC. CBDV and CBGA were not able to induce any change in ERK phosphorylation. In $CB_{1/2}RHet$-expressing cells Δ^9-THC, CBD and, to a minor extent, CBGV did lead to ERK phosphorylation induction. CBDA, CBGA and CBG compounds displayed similar potency and slightly different maximal effect, which was lower

than that of the other compounds. CBDV and CBG exerted the lowest effect in potency and maximal effect of all phytocannabinoids at 1 μM concentration.

Differential results were obtained in label-free DMR recordings in cells expressing CB_1R or CB_2R although all compounds behaved similarly in cells coexpressing the two receptors (Fig. 4C,G,K). It is important to note that in these recordings the effects are only observed for all compounds at the higher concentrations, starting at 100 nM and increasing to 10 μM.

Finally, results from β-arrestin recruitment experiments were qualitatively and/or quantitatively different to those obtained when other signaling outputs were measured. A common trend was the negligible effect of CBGA over CB_1R or CB_2R; when the two receptors were expressed CBGA was able to recruit ß-arrestin 2 at relatively low concentrations although he maximal effect was still low (Fig. 4E,H,L). In CB_1R-expressing cells CBGV displays similar potency and maximal effect to those of the reference phytocannabinoid Δ^9-THC in the increase of β-arrestin recruitment. All the other phytocannabinoids display similar maximal effect, smaller than the Δ^9-THC effect, but different potency in increasing β-arrestin recruitment, being CBDA the more potent and CBGA the less potent of them. In CB_2R-expressing cells all phytocannabinoids display similar potency and maximal effect, always less potent than the reference phytocannabinoid Δ^9-THC in the increase of β-arrestin recruitment, in addition CBGA was not able to induce any β-arrestin recruitment. Similar results to those in CB_2R-expressing cells were observed in the $CB_{1/2}$RHet-expressing cells in the β-arrestin recruitment but the different phytocannabinoids exert different potencies, being CBDA the most potent and CBGA the less, as observed in the CB_1R-expressing cells.

Taking together the binding and the signaling results, it is derived that there is a biased signaling, i.e. depending on the binding mode and on the receptor differential functional effects are exerted by the different phytocannabinoids. Accordingly, our next objective was to calculate the bias factor for each compound on the CB_1R, the CB_2R and the $CB_{1/2}$RHet. A further possibility that was also explored is whether some of the phytocannabinoids here studied may behave as agonist, inverse agonists or even as neutral antagonists.

Analysis of biased agonism

To better understand cannabinoid receptor pharmacology, it is convenient to analyze different signaling pathways. In fact, GPCR ligands show functional selectivity [49,50]; therefore, activation of cannabinoid receptors may engage different cytocrin[51] signaling pathways and the question is whether this might already occur using natural phytocannabinoids.

For biased agonism assessment, HEK-293T cells expressing CB_1R, CB_2R or $CB_{1/2}$RHets, were treated with CBG, CBGA, CBGV, CBD, CBDA, CBDV or Δ^9-THC and four different functional readouts were analyzed: cAMP levels, ERK1/2 phosphorylation, ß-arrestin-2 recruitment and dynamic mass redistribution (DMR). In all cases CBD was the compound

of reference. The functional response used as reference to calculate the bias factor was the effect on forskolin-induced intracellular cAMP levels.

In the radar plot showing bias factors for CB_1R-expressing cells it can be observed that CBDA is biased to ß-arrestin recruitment with a marked inability to activate the MAPK pathway (Fig. 5A). CBDV also led to negligible MAPK pathway activation but ß-arrestin recruitment was comparable to that obtained with CBD (Fig. 5A). On the other hand, CBGV showed a balanced behavior in between CBG and Δ^9-THC showing agonistic behavior that can define CBGV as probably psychotropic. CBGA showed a similar behavior as that of CBG, with inferior values of bias factors and being unable to recruit ß-arrestin-2. The pattern of biased agonism was fairly different in CB_2R-expressing cells. Many of the tested compounds were biased towards the MAPK signaling pathway and CBGA was the only compound with little capacity to recruit ß-arrestin-2 and to activate MAPK signaling (Fig. 5B).

We found a differential bias pattern in cells expressing $CB_{1/2}$RHets. CBDA and CBDV were biased towards ß-arrestin-mediated signaling, i.e. there was not any compound ineffective in achieving ß-arrestin 2 recruitment. CBGV showed similar behavior to that of CBG although differing in the value of the respective bias factor, and CBGA was little biased towards MAPK signaling (Fig. 5C).

Figure 5

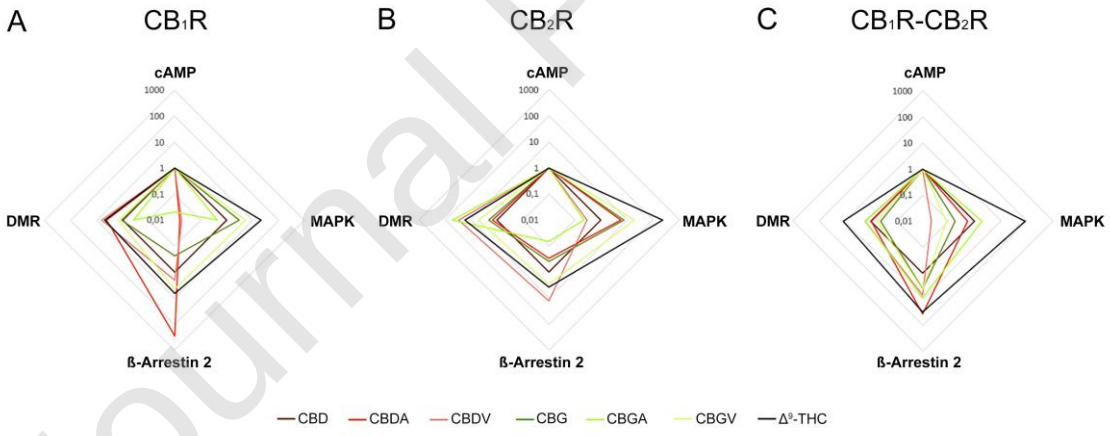

Figure 5. Biased agonism on CB_1R, CB_2R and $CB_{1/2}$RHets

Radar plots showing the bias factors of the CBD, CBDA, CBDV, CBG, CBGA, CBGV and Δ^9-THC in cAMP, MAPK, DMR and β-arrestin recruitment functional outcomes in HEK-

293T cells expressing CB_1R (A), CB_2R (B) or both (C). In all cases, the compound of reference was CBD and the response of reference was forskolin-induced cAMP production.

Assessment of antagonism

Considering all signaling data we questioned about a possible role of tested phytocannabinoids as either neutral antagonists or inverse agonists. First, the cAMP-PKA signaling was analyzed in HEK-293T cells expressing CB_1R and treated with increasing concentrations of the selective CB_1R agonist, ACEA, in the presence of 1 μM concentration of either CBGA, CBGV, CBD, CBDA or CBDV (Fig. 6A). The main observation was that when analyzing cAMP intracellular levels, CBGA and CBDA, in less magnitude, shifted to the right the dose-response curve. This observation may reflect inverse agonism or negative allosteric modulation. We observed that CBGV can produce a moderated shift to the left of the dose response curve of the ACEA. We suspect that is not a real shift to the left of the dose-response curve of the ACEA, because the dose-response curve observed is very similar to the effects of CBGV alone (Fig. 4A). Then, more than a positive allosteric effect of the CBGV over the ACEA effect, we propose that CBGV is acting as an agonist on the orthosteric pocket of CB_1 receptor and ACEA is not able to displace it.

cAMP-PKA signaling analyzed in HEK-293T cells expressing CB_2R and treated with increasing concentrations of the selective CB_2R agonist, JHW133, in the presence of 1μM concentration of either CBG, CBGA, CBGV, CBD, CBDA or CBDV (Fig. 6B) led to identifying that CBDA, CBGA and CBD shifted the dose-response curve to the right, reflecting inverse agonism or negative allosteric modulation.

Finally, in cells expressing both CB_1 and CB_2 receptors, none of the compounds significantly reverted the effect of the non-selective agonist, CP55490 (Fig. 6C). Only CBDA was able to shift little to the right the dose -response curve of CP55490, indicating inverse agonism or negative allosteric modulation. It should be however noted that the effect of CP-55940 in cells expressing $CB_{1/2}$RHets was small in magnitude. Interestingly, we observe that CBD and CBGV can shift to the left the dose response curve of the CP55490, indicating a possible positive allosteric modulation of this phytocannabinoids over $CB_{1/2}$RHets. In the case of the CBGV the dose-response curve of CP55490 + CBGV is similar to the dose-response curve of the CBGV alone in the cells expressing $CB_{1/2}$RHets (Fig. 4I). Then, our observations seem to indicate that CBGV is acting as an agonist upon binding to the orthosteric pocket of CB_1 receptor of the $CB_{1/2}$RHets and CP55490 is not able to displace it.

Figure 6

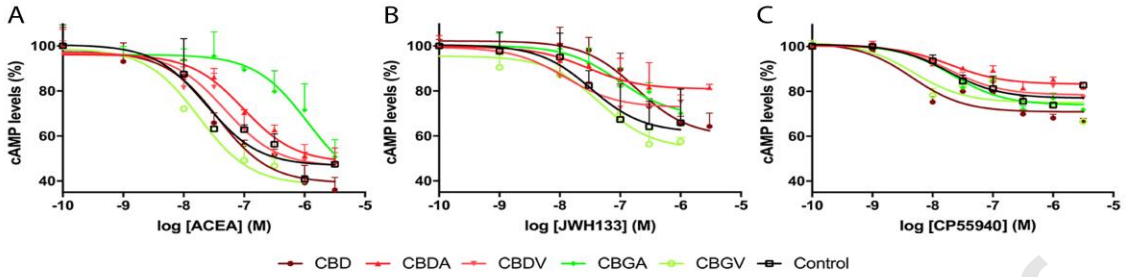

Figure 6. Effect of CBDA, CBDV, CBGA or CBGV on the effects induced by CB_1R, or CB_2R agonists.

HEK-293T cells expressing CB_1R (0.75 μg cDNA) (A), CB_2R (1 μg cDNA) (B) or both (C) were treated with 1 μM of CBD, CBDA, CBDV, CBGA, CBGV or vehicle 15 min before addition of the selective CB_1R (ACEA) or CB_2R (JWH133) agonist, or the non-selective agonist CP55940. Dose–response curves for decreases in forskolin-induced cAMP production using ACEA to induce CB_1R activation, JWH133 to induce CB_2R activation or CP55940 to activate both CB_1 and CB_2 and heterodimers of receptors were analyzed and data are expressed in % respect to the effect of forskolin (0.5 μM, 100 %). Data represent the mean ± SEM (n = 6 in triplicates).

Discussion

In this paper we provide pharmacological data of varinic and acidic CBD-type and CBG-type phytocannabinoids on CB_1 and CB_2 cannabinoid receptors, either individually expressed or forming $CB_{1/2}$RHet complexes. The latter is of interest as these complexes are expressed, among other, in pallidal neurons [52] and microglial cells [9]. Interestingly, $CB_{1/2}$RHets mediate in activated microglia some of the proven neuroprotective effects of cannabinoids [9].

Different conclusions may be drawn from the results using compounds with limited variations of the pharmacophore and different binding modes using both isolated membranes and living cells. Using [^{3}H]-CP-55940 the first interesting finding is that all compounds behave similarly in either CB_1R or CB_2R. Using the same radioligand in a different membrane preparation, Rosenthaler et al., [45] showed roughly similar behavior of CBD and CBG in either CB_1 or CB_2 receptors. In contrast, the K_i values of CBDV for binding to CB_1R and CB_2R were reported to be 14,7 μM and 574 nM, respectively. It is not readily evident why we find similar values of K_i in competing the binding to either receptors

while the K_i values for binding to CB_1R binding reported by Rosenthaler et al., [45] and by us (14,4 μM, table 1) are very similar.

~~Compounds with more affinity, in general, are the neutral ones; until then,~~ The compound with more affinity for cannabinoid receptors was CBDA. CBGA and CBDV have a very low affinity for both CB_1R and CB_2R using [^{3}H]-CP-55940 as ligand. It is also noticeable that just by removing an ethyl group of the lateral alkyl chain, converting neutral into varinic phytocannabinoids, the affinity worsens by an order of magnitude in CBDV respect to CBD, but not in CBGV compared to CBG. Using [^{3}H]-WIN-55,212-2 the binding to the CB_1R was "lost", thus showing that nonselective agonists, [^{3}H]-WIN-55,212-2 and [^{3}H]-CP-55940, sit differently in the orthosteric center of the CB_1R. This apparent loss of binding was anticipated by [32] who, using the same radioligand, showed that the K_i value for CBG in membranes expressing the human CB_1R was >60,000 nM while the K_i value for CBG in membranes expressing the human CB_2R was in the micromolar range but measurable (16,075 ± 4,835 nM). In fact, using [^{3}H]-WIN-55,212-2 the results of the binding to the CB_2R were very similar to those found using [^{3}H]-CP-55940 ~~for all phytocannabinoids~~. The binding to living cells using a homogeneous assay, which at present is only possible in the case of the CB_2R, led to results that were similar to those found using [^{3}H]-CP-55940 but with the difference that CBGV was the compound with more affinity while CBDA displayed less affinity for CB_2R than CBD. ~~Other difference, namely~~Removal of the ethyl group of CBD, to obtain CBDV, did not significantly modify the affinity.

Noticeable was the differential binding of CBDA in cells expressing CB_2R versus cells coexpressing the two receptors in the HTRF competition binding experiments. Right after the discovery of GPCR heterodimers around year 2000, scientists considered that variations in affinity were reflecting allosteric changes induced by the partner receptor in a GPCR heteromer. To our knowledge, the first report showing significant variation of affinity parameters in the binding to a receptor forming heteromers focused on the 5-HT_{2A}/metabotropic glutamate 2 receptor interaction [53]. Moreover, the serotonin receptor 5-HT_{2A} agonist-induced [^{35}S]-GTP-γS-binding was diminished upon interacting with the metabotropic glutamate 2 receptor. Now the view is that the structure of receptors in heteromers and receptor functionality is different than in monomers but that the binding affinity may be similar [54–56]. In the results here presented, affinity changed (significantly) only in the case of CBDA, while rest of phytocannabinoids displayed similar affinities in the heteromeric context. For many heteromers, the variation in K_D/K_i values is minor, i.e. affinity variations are not considered of physiological relevance for GPCR heteromers.

Functional assays showed that, despite the negligible competition of the [^{3}H]-WIN-55,212-2 binding to the CB_1R, tested phytocannabinoids were able to target the receptor and act as agonists. They also behaved as agonists of the CB_2R and engaged receptors in the heteromeric context. Signaling outputs were always consistent with agonism displaying, obviously, different patterns of potency and maximal effect. This hypothesis was confirmed by the lack of antagonism as deduced from the results of Fig. 6. Therefore, what it may happen when a given phytocannabinoid is *in vivo* acting is not neutral antagonism but ~~not~~ inverse agonism or allosteric modulation.

~~Overall, many of the phytocannabinoids here tested were previously time ago considered as either partial agonist or inverse antagonists. However,~~ Our data also show that phytocannabinoids lead to biased agonism at both CB_1 and CB_2 receptors. In fact, affinity determined by competition binding was not directly related to potency and/or maximal effect. Biased agonism was first noticed by the dose-response curves in the four signaling outputs that were analyzed. Further calculation of bias factors (Fig. 5) led to confirm that each phytocannabinoid behaved differently thus providing a compelling example of biased signaling. By removing/adding an ethyl group in the alkyl chain or by a differential decoration, carboxylic acid group, of the main core the response is qualitatively and/or quantitively different. It should be noted that CBD was chosen as reference compound knowing that it is able to bind to both orthosteric and allosteric centers [24,25]. Remarkably, recent data on the crystal structure of melatonin MT_1 and MT_2 receptors show an "*intramembrane ligand entry* (of agonists to the orthosteric site) *in both receptors*" [57,58]. More importantly, a bitopic compound that was symmetrical, i.e. having two identical pharmacophores at each side, find its way to the MT_1 receptor, i.e. the pharmacophore binds to two different sites [58]. Recent elucidation of the 3D structure of the CB_2R [23] indicates that agonist binding to the CB_2R may be similar to that reported for the bitopic ligand of the MT_1 receptor. In fact, we have data suggesting that the CB_2R may have a non-orthosteric site where structures that go into the orthosteric site may also bind (Morales et al., in preparation). Going back to the biased signaling exerted by phytocannabinoids, it is confirmed that Δ^9-THC is unable to significantly engage Gi protein/cAMP/PKA pathway in CB_2R and similarly, CBG had low potency of activating Gi-proteins, especially when acting on individual receptors. In contrast Δ^9-THC, and also CBGV via CB_1 and in less potency via CB_2 receptors were able to significantly activate the MAPK signaling pathway and recruit ß-arrestins. The results fit with the hypothesis of some compounds more prone to engage Gi than to enhancing ERK1/2 phosphorylation and/or ß-arresting recruitment while other were more prone to enhance ERK1/2 phosphorylation and/or ß-arresting recruitment than to engaging Gi. We consider CBGV data as an example of complex behavior that can be summarized as providing both Gi and MAPK pathway activation, therefore acting as a potent agonist. On the one hand MAPK pathway activation via CB_1R, which is similar to that of Δ^9-THC, opens the question on whether CBGV has or has not psychotropic potential. On the other hand, data in Fig. 6 shows that CBGV would in vivo act as a competitor of endocannabinoids, i.e. as inverse agonist of cannabinoid receptors. In addition, these results and our previous results using other cannabinoids [24,46,59] suggest that biased signaling is more a question of the conformations acquired by cannabinoid receptors upon ligand binding than to a landscape of conformations waiting for the binding of the "right" compound. We think that the limited chemical variations of natural cannabinoids can be correlated with the binding behavior in the different setups/ligands and with bias factors and/or with potency and maximal effect to provide information of the structural changes that lead to a specific functional output. Our data together with the myriad of already available structure/activity data on natural and synthetic cannabinoids (rigorously compiled in [60]) and the recent availability of crystal structures for both CB_1 and CB_2 receptors [20–23] may provide a significant advance in the design of chemical structures with

therapeutic potential and with few side effects. We consider specially relevant the very recent release of the cryo-Electron Microscopy structure of the active CB_2R-G_i complex [61].

Materials and Methods

Reagents

ACEA, JWH133 and CP55,490 were purchased from Tocris Bioscience (Bristol, UK), CBD, CBDA, CBDV, CBG, CBGA, CBGV and Δ^9-THC were obtained as described below. Chemical structures for CBG, CBGA, CBGV, CBD, CBDA and CBDV are shown in Supplementary Fig. S1. The CB_2R agonist 3-[[4-[2-tert-butyl-1-(tetrahydropyran-4-ylmethyl)benzimidazol-5-yl]sulfonyl-2-pyridyl]oxy]propan-1-amine (CM157) conjugated to a fluorescent probe was developed in collaboration with Cisbio Bioassays (see [47]). Δ^9-THC was provided by Phytoplant Research with all permissions required under Spanish and European laws and only for non-human investigation purposes.

Cannabinoid isolation and purification

CBD was purified from the Cannabis variety SARA (CPVO/20150098), CBG and CBGA from the variety AIDA (CPVO/20160167) following a previously described direct crystallization method (Nadal, 2016; patent US9765000B2; EP3247371B1; WO2016116628A1) that provides compounds with >95% purity. CBDA was purified from the Cannabis variety SARA (CPVO/20150098), CBDV from the variety THERESA (CPVO/20160116), CBGV from the variety JUANI (CPVO/20160117) and Δ^9-THC from the variety MONIEK (CPVO/20160114) following a previously described liquid-liquid chromatography method (Nadal, 2018; patent US102007199B2; WO201914552A1) that provides compounds with >95% purity. For purity analysis an Agilent liquid chromatography set-up (Model 1260, Pittsburgh, PA, USA) consisting of a binary pump, a vacuum degasser, a column oven, an autosampler and a diode array detector (DAD) equipped with a 150 mm length x 2.1 mm internal diameter, 2.7 μm pore size Poroshell 120 EC-C18 column was used. The analysis was performed using water and acetonitrile both containing ammonium formate 50 mM as mobile phases. Flow rate was 0.2 mL/min and the injection volume was 3 μL. Chromatographic peaks were recorded at 210 nm. All determinations were carried out at 35ºC. All samples were analyzed in duplicate. The results of each cannabinoid were calculated as weight (%) versus a commercial standard, except for CBGV, whose purity was calculated as % of total peak area because there is no commercial standard available. CBD batch nº L01258-M-1.0, CBDA batch n° L01221-M-1.0, CBGV batch nº L01260-M-1.0 and Δ^9-THC batch nº L01201-M-0.1 were purchased from THCpharm, (Frankfurt, Germany). CBDV batch n° FE06071601, CBG batch n° FE08031502 and CBGA batch n° FE06061603 were purchased from Cerilliant (Round Rock, Texas). The purity of each compound isolated and used in the study was CBD = 96,04%, CBDA >100%, CBDV = 100,0%, CBG >100%, CBGA = 95,69%, CBGV = 98,05% (peak area) and Δ^9-THC = 95,51%.

Expression vectors

cDNAs for the human version of cannabinoid CB_1, CB_2 and dopamine D_1 receptors lacking the stop codon were obtained by PCR and subcloned to a RLuc-containing vector (p*RLuc*-N1; PerkinElmer, Wellesley, MA) using sense and antisense primers harboring unique restriction sites for HindIII and BamHI or subcloned to a pEYFP-containing vector (pEYFP-N1; Clontech, Heidelberg, Germany) or a p-GFP^2–containing vector (Clontech, Heidelberg, Germany) using sense and antisense primers harboring unique restriction sites for BamHI and KpnI generating CB_1R-Rluc, CB_2R-Rluc, CB_1R-YFP, CB_2R-YFP, D_1R-GFP^2 and CB_2R-GFP^2 fusion proteins.

Cell culture and transfection

HEK-293T cells were grown in DMEM medium (Gibco, Paisley, Scotland, UK) supplemented with 2 mM L-glutamine, 100 U/mL penicillin/streptomycin, MEM Non-Essential Amino Acids Solution (1/100) and 5% (v/v) heat inactivated Fetal Bovine Serum (FBS) (Invitrogen, Paisley, Scotland, UK). Cells were maintained in a humid atmosphere of 5% CO_2 (37º). Cells were transiently transfected using PEI (Polyethyleneimine, Sigma, St. Louis, MO, USA) as previously described [62] and used for functional assays 48 h after (unless otherwise stated). Number of passages was <12 and cells were tested to confirm lack of mycobacterial infection.

For radioligand binding experiments CHO cells, stably transfected with cDNA for human CB_1 or CB_2 cannabinoid receptors, were grown adherently and maintained in Ham's F12 containing 10% fetal bovine serum, penicillin (100 U/mL), streptomycin (100 µg/mL) and geneticin (G418, 0.4 mg/mL) at 37° in a humid atmosphere of 5% CO_2.

Immunocytochemistry assays

HEK-293T cells expressing CB_1R-YFP and CB_2R-Rluc, treated for 30 min with CBD, CBDA, CBDV, CBG, CBGA, CBGV, Δ^9-THC or vehicle were fixed in 4% paraformaldehyde for 15 min and washed twice with PBS containing 20 mM glycine before permeabilization with PBS-glycine containing 0.2% Triton X-100 (5 min incubation). Cells were treated for 1 h with PBS containing 1% bovine serum albumin and labelled with a primary mouse anti-RLuc (1/100; Millipore (Darmstadt, Germany)) antibody, and subsequently treated for 1 h with an anti-rabbit (1/200; Jackson ImmunoResearch) Cy3-conjugated secondary antibody IgG (red). Samples were washed several times and mounted with 30% Mowiol (Calbiochem). Samples were observed in a Leica SP2 confocal microscope (Leica Microsystems). The CB_1R-YFP expression was detected by the own fluorescence of the YFP (green).

Bioluminescence Resonance Energy Transfer (BRET)

HEK-293T cells were transiently cotransfected with a constant amount of cDNA encoding for CB_1-RLuc and with increasing amounts of cDNA corresponding to either CB_2- or D_1-GFP^2 (as negative control). To analyze cannabinoid compounds induced effect, HEK-293T cells were transiently cotransfected with a constant amount of cDNA encoding for CB_1-RLuc and CB_2R-GFP^2 to obtain a maximum BRET value. 48 h after transfection cell suspension was adjusted to 20 µg of protein using a Bradford assay kit (Bio-Rad, Munich, Germany) using bovine serum albumin for standardization. Cannabinoid compound

treatment was performed 10 minutes prior to each quantification. To quantify protein-GFP^2 expression, fluorescence was read in a FluoStar Optima Fluorimeter (BMG Labtechnologies, Offenburg, Germany) equipped with a high-energy xenon flash lamp, using a 10 nm bandwidth excitation filter and reading at 410 nm. For BRET measurements, readings were collected 30 seconds after the addition of 5 μM DeepBlueC (Molecular Probes, Eugene, OR) using a Mithras LB 940, which allows the integration of the signals detected in the short-wavelength filter at 415 nm and the long-wavelength filter at 510 nm. To quantify protein-RLuc expression, luminescence readings were performed 10 min after 5 μM coelenterazine H addition using a Mithras LB 940. The net BRET is defined as [(long-wavelength emission)/(short-wavelength emission)]-C_f, where C_f corresponds to [(long-wavelength emission)/(short-wavelength emission)] for the donor construct expressed alone in the same experiment. GraphPad Prism software (San Diego, CA, USA) was used to fit data. BRET is expressed as milli BRET units, mBU (net BRET x 1,000).

Radioligand competition binding experiments

Membranes from transfected CHO cells were prepared from cells washed with PBS and scraped off plates in ice-cold hypotonic buffer (5 mM Tris HCl, 2 mM EDTA, pH 7.4). The suspension was treated with a Polytron and then centrifuged for 30 min at 40,000 x g. Competition binding experiments were performed incubating 0.3 nM of [^{3}H]-CP-55940 or 3 nM of [^{3}H]-WIN-55,212-2 and different concentrations of the tested compounds with membranes obtained from CHO cells expressing human CB_1 or CB_2 receptors (10 μg protein/ sample) for 90 min (CB_1R) or 60 min (CB_2R) at 30°. Non-specific binding was determined in the presence of 1 μM WIN-55,212-2. Bound and free radioactivity were separated by filtering, and filter-bound radioactivity was counted using a Packard Tri Carb 2810 TR scintillation counter (Perkin Elmer).

Homogeneous competition binding assays

SNAP CB_2R were expressed in HEK-293T cells using the elsewhere-described procedure[24]. For SNAP protein labeling, cell culture medium was removed from the 25-cm^2 flask and 100 nM SNAP-Lumi4-Tb, previously diluted in 3 mL of TLB 1X, was added to the flask and incubated for 1 hour at 37°C under 5% CO_2 atmosphere in a cell incubator. Cells were then washed four times with 2 mL of TLB 1X to remove the excess of SNAP-Lumi4-Tb, detached with enzyme-free cell dissociation buffer, centrifuged 5 min at 1,500 rpm and collected in 1 mL of TLB 1X. Tag-lite-based binding assays were performed 24 hours after transfection. Densities of 2,500-3,000 cells/well were used to perform binding assays in white opaque 384-well plates.

For competition binding assays, the fluorophore-conjugated CB_2R ligand (labeled CM157), CBD, CBDA, CBDV, CBG, CBGA and CBGV were diluted in TLB 1X. HEK-293T cells transiently expressing Tb-labeled SNAP-CB_2R with or without CB_1R were incubated with 20 nM fluorophore-conjugated CB_2R ligand, in the presence of increasing concentrations (0-10 μM range) of cannabinoid compounds. Plates were then incubated for at least 2 h at room temperature before signal detection. Homogeneous time-resolved fluorescence energy transfer (HTRF) was detected using a PHERAstar Flagship microplate reader (Perkin-Elmer,

Waltham, MA, USA) equipped with a FRET optic module allowing donor excitation at 337 nm and signal collection at both 665 and 620 nm.

cAMP determination

Two hours before initiating the experiment, HEK-293T cells medium was replaced by serum-starved DMEM medium. Then, cells were detached and resuspended in DMEM medium containing 50 μM zardaverine. Then, cells were plated in 384-well microplates (2,500 cells/well), pretreated (15 min) with the corresponding antagonists -or vehicle- and stimulated with agonists (15 min) before adding 0.5 μM forskolin or vehicle. Readings were performed after 60 min incubation at 25º. Homogeneous time-resolved fluorescence energy transfer (HTRF) measures were performed using the Lance Ultra cAMP kit (PerkinElmer, Waltham, MA, USA). Fluorescence at 665 nm was analyzed on a PHERAstar Flagship microplate reader equipped with an HTRF optical module (BMG Lab technologies, Offenburg, Germany).

ERK phosphorylation assays

To determine ERK1/2 phosphorylation, 40,000 cells/well were plated in transparent Deltalab 96-well microplates and kept at the incubator for 24 h. 2 to 4 h before the experiment, the medium was substituted by serum-starved DMEM medium. Then, cells were stimulated at 25°C for 7 min with compounds or vehicle in serum-starved DMEM medium. Cells were then washed twice with cold PBS before addition of lysis buffer (20 min treatment). 10 μL of each supernatant were placed in white ProxiPlate 384-well microplates and ERK 1/2 phosphorylation was determined using AlphaScreen®SureFire® kit (Perkin Elmer) following the instructions of the supplier and using an EnSpire® Multimode Plate Reader (PerkinElmer, Waltham, MA, USA).

Dynamic mass redistribution (DMR) assays

Cell mass redistribution induced upon receptor activation was detected by illuminating the underside of a biosensor with polychromatic light and measuring the changes in the wavelength of the reflected monochromatic light, that is a function of the index of refraction. The magnitude of this wavelength shift (in picometers) is directly proportional to the amount of DMR. HEK-293T cells expressing CB_1R, CB_2R or both were seeded in 384-well sensor microplates to obtain 70-80% confluent monolayers constituted by approximately 10,000 cells per well. Previous to the assay, cells were washed twice with assay buffer (HBSS with 20 mM HEPES, pH 7.15) and incubated 2 h with assay-buffer containing 0.1% DMSO (24°C, 30 μL/well). Hereafter, the sensor plate was scanned and a baseline optical signature was recorded for 10 min before adding, where indicated, 10 μl of an antagonist for 30 min followed by the addition, of 10 μL of the tested compounds (diluted in assay buffer). DMR recordings were made in an EnSpire® Multimode Plate Reader (PerkinElmer, Waltham, MA, USA) by a label-free technology. Then, DMR responses were monitored for at least 5,000 s. Results were analyzed using EnSpire Workstation Software v 4.10.

β-arrestin 2 recruitment

β-arrestin recruitment was determined as previously described [63]. Briefly, BRET experiments were performed in HEK-293T cells 48h after transfection with the cDNA for either CB_1R-YFP, CB_2R-YFP or CB_2R-YFP and CB_1R, and 1 μg cDNA corresponding to β-arrestin 2-RLuc. Cells (20 μg protein) were distributed in 96-well microplates (Corning 3600, white plates with white bottom) and incubated with compounds for 10 min prior to the addition of 5 μM coelenterazine H (Molecular Probes, Eugene, OR). 1 min after coelenterazine H addition, BRET readings corresponding to β-arrestin 2-Rluc and receptor-YFP were quantified. The readings were collected using a Mithras LB 940 (Berthold Technologies, Bad Wildbad, Germany) that allows the integration of the signals detected in the short-wavelength filter at 485 nm and the long-wavelength filter at 530 nm. To quantify protein-RLuc expression, luminescence readings were performed 10 min after addition of 5 μM coelenterazine H.

Calculation of bias factor

Using the operational model described by J.W. Black et al. and according to Rajagopal et al., [64] the bias factor "*quantifies the relative stabilization of one signaling state over another compared with a selected reference agonist*" and the formula to calculate bias factor "bias" is: $bias = 10^{\Delta\Delta\log(\tau/K_A)_{j1-j2}}$ and $log\ bias = \Delta\log(\tau/K_A)_{j1} - \Delta\log(\tau/K_A)_{j2}$, in which j_i denotes one of the analyzed pathways/responses (here j_1, j_2, j_3 and j_4, because four different responses were measured). The pathway of reference was the canonical for G_i, i.e. j_1 refers to cAMP level determinations. τ denotes the maximum value in each response and K_A is the antilogarithm of half maximal effective concentration: EC_{50} if the agonist provides a direct response or IC_{50} if the agonist provides a reduction of the response provided by another reagent (for instance forskolin in cAMP level determination assays).

Data handling and statistical analysis

Data was analyzed in a blinded way, i.e. the investigator responsible for data analysis did not know which results came from controls and which results came from treatments. Based on previous experience using outlier detection tests, all data were included in the analysis.

Affinity values (K_i) were calculated from the IC_{50} obtained in competition radioligand binding assays according to the Cheng and Prusoff equation: $K_i = IC_{50}/(1 + [C]/K_D)$, where [C] is the free concentration of the radioligand and K_D its dissociation constant. [65].

Data from homogeneous binding assays were analyzed using Prism 6 (GraphPad Software, Inc., San Diego, CA). K_D values were obtained from saturation curves of the specific binding. Specific binding was determined by subtracting the non-specific HTRF ratio from the total HTRF ratio. K_D and B_{max} values were calculated assuming one binding site in monomeric receptor. Unlike in radioligand binding assays, B_{max} values obtained from HTRF data do not reflect absolute values of receptor binding sites; they are however useful for comparison purposes. As in radioligand binding assays, K_i values were determined according to the Cheng and Prusoff equation [65]. Signal-to-background (S/B ratio) calculations were performed by dividing the mean of the maximum value (μ_{max}) by that of the minimum value (μ_{min}) obtained from the sigmoid fits.

The data are shown as the mean ± SEM. Statistical analysis was performed with SPSS 18.0 software. The test of Kolmogorov-Smirnov with the correction of Lilliefors was used to evaluate normal distribution and the test of Levene to evaluate the homogeneity of variance. Significance was analyzed by one-way ANOVA, followed by Bonferroni's multiple comparison *post hoc* test. Significant differences were considered when $p<0.05$.

Conflict of interests

GN, KV, AL, FV, RRS, IR, IRR, PAB, MC, AND RF declare no conflict of interests.

CFV and VSM declare that they work for Phytoplant Research SL, a research company that does not directly sell any product (web page: https://www.phytoplantresearch.com/). XN worked for Phytoplant Research SL and is not currently linked to the company. Neither CFV, VSM nor XN have shares of Phytoplant Research SL or any cannabinoid-related for-profit company.

Author Contributions:

RF, GN, VSM and XN designed and supervised the research; they coordinated the work in the different laboratories. GN, AL, IR, RRS and IRR performed homogeneous binding and signaling experiments, provided raw data and participated in data analysis. PAB, FV and KV performed radioligand binding assays and provided binding parameters. VSM and XN isolated the cannabinoid compounds, CFV performed analytical purity determinations of phytocannabinoids. RF and GN prepared a first version, VSM and XN revised it and prepared a second version that was subsequently edited by GN, PAB, KV, AL, IR, RRS, IRR, and CFV. All authors have given approval to the final version of the manuscript.

Acknowledgements

Funding sources: Spanish Ministerio de Economía y Competitividad (MINECO) #BFU2015-64405-R, SAF2017-84117-R and #RTI2018-094204 grants (they may include EU FEDER funds) and Alzheimer's Association grant AARFD-17-503612.

Table 1. K_i values for competition binding using radiolabeled ligands. Displayed data correspond to binding to membranes expressing either the CB_1R or the CB_2R.

	[^{3}H]-CP 55940	**[^{3}H]-CP 55940**	**[^{3}H]-WIN 55,212-2**	**[^{3}H]-WIN 55,212-2**
Compound	**CB_1R– K_i (nM)**	**CB_2R – K_i (nM)**	**CB_1R – K_i (nM)**	**CB_2R – K_i (nM)**
WIN 55,212-2	8.08 ± 0.65	3.22 ± 0.31	9.86 ± 0.84	3.48 ± 0.27
CBD	1,690 ± 110	1,714 ± 70	>30,000	4,019 ± 342
CBG	1,045 ± 74	1,225 ± 85	>30,000	2,656 ± 130
CBDA	626 ± 52	813 ± 62	>30,000	2,434 ± 142
CBGA	13,116 ± 1047	17,348 ± 987	>30,000	>30,000
CBDV	14,445 ± 999	15,719 ± 975	>30,000	>30,000
CBGV	2,865 ± 160	3,005 ± 127	>30,000	8,089 ± 769

Table 2. K_i values for competition binding using the HTRF technique with a fluorophore-conjugated selective CB_2R ligand. Displayed data correspond to binding to living HEK-293T cells expressing the CB_2 or CB_2 and CB_1 receptors. Note that, in both cases, the binding parameters correspond to the binding to the CB_2R.

	CM157 red ligand	**CM157 red ligand**
Compound	**CB_2R – K_i (nM)**	**CB_2R (+ CB1)– K_i (nM)**
CBD	705± 40.7	324 ± 45.3
CBG	205 ± 29.6	135 ± 19.9
CBDA	354 ± 30.0	4,530 ± 83.2
CBGA	2,958 ± 59.1	2,958 ± 73.2
CBDV	3,088 ± 57.9	3,088 ± 57.9
CBGV	162 ± 25.1	162 ± 25.1

References

[1] R. Mechoulam, Cannabis - The Israeli perspective, J. Basic Clin. Physiol. Pharmacol. 27 (2016) 181–187. doi:10.1515/jbcpp-2015-0091.

[2] Perras C, Sativex for the management of multiple sclerosis symptoms., Issues Emerg. Health Technol. 72 (2005) 1–4. http://www.ncbi.nlm.nih.gov/pubmed/16317825 (accessed August 4, 2018).

[3] R. Mechoulam, M. Spatz, E. Shohami, Endocannabinoids and neuroprotection, Sci. STKE Signal Transduct. Knowl. Environ. 2002 (2002) re5. doi:10.1126/stke.2002.129.re5.

[4] D.I. Brierley, J.R. Harman, N. Giallourou, E. Leishman, A.E. Roashan, B.A.D. Mellows, H.B. Bradshaw, J.R. Swann, K. Patel, B.J. Whalley, C.M. Williams, Chemotherapy-induced cachexia dysregulates hypothalamic and systemic lipoamines and is attenuated by cannabigerol, J. Cachexia. Sarcopenia Muscle. (2019) jcsm.12426. doi:10.1002/jcsm.12426.

[5] V. Di Marzo, F. Piscitelli, R. Mechoulam, Cannabinoids and Endocannabinoids in Metabolic Disorders with Focus on Diabetes, in: Handb. Exp. Pharmacol., 2011: pp. 75–104. doi:10.1007/978-3-642-17214-4_4.

[6] L.O. Hanuš, S.M. Meyer, E. Muñoz, O. Taglialatela-Scafati, G. Appendino, Phytocannabinoids: A unified critical inventory, Nat. Prod. Rep. 33 (2016) 1357–1392. doi:10.1039/c6np00074f.

[7] G. Fournier, C. Richez-Dumanois, J. Duvezin, J.-P. Mathieu, M. Paris, Identification of a New Chemotype in *Cannabis sativa* : Cannabigerol - Dominant Plants, Biogenetic and Agronomic Prospects, Planta Med. 53 (1987) 277–280. doi:10.1055/s-2006-962705.

[8] L. Callén, E. Moreno, P. Barroso-Chinea, D. Moreno-Delgado, A. Cortés, J. Mallol, V. Casadó, J.L. Lanciego, R. Franco, C. Lluis, E.I. Canela, P.J. McCormick, Cannabinoid receptors CB1 and CB2 form functional heteromers in brain., J. Biol. Chem. 287 (2012) 20851–65. doi:10.1074/jbc.M111.335273.

[9] G. Navarro, D. Borroto-Escuela, E. Angelats, I. Etayo, I. Reyes-Resina, M. Pulido-Salgado, A. Rodríguez-Pérez, E. Canela, J. Saura, J.L. Lanciego, J.L. Labandeira-García, C.A. Saura, K. Fuxe, R. Franco, A.I. Rodriguez-Perez, E.I. Canela, J. Saura, J. Lanciego, J. Labandeira-García, C. Saura, K. Fuxe, R. Franco, Receptor-heteromer mediated regulation of endocannabinoid signaling in activated microglia. Relevance for Alzheimer's disease and levo-dopa-induced dyskinesia, Brain. Behav. Immun. 67 (2018) 139–151. doi:10.1016/j.bbi.2017.08.015.

[10] F.A. Iannotti, C.L. Hill, A. Leo, A. Alhusaini, C. Soubrane, E. Mazzarella, E. Russo, B.J. Whalley, V. Di Marzo, G.J. Stephens, Nonpsychotropic Plant Cannabinoids,

Cannabidivarin (CBDV) and Cannabidiol (CBD), Activate and Desensitize Transient Receptor Potential Vanilloid 1 (TRPV1) Channels in Vitro: Potential for the Treatment of Neuronal Hyperexcitability, ACS Chem. Neurosci. 5 (2014) 1131–1141. doi:10.1021/cn5000524.

[11] E. D'Aniello, T. Fellous, F.A. Iannotti, A. Gentile, M. Allarà, F. Balestrieri, R. Gray, P. Amodeo, R.M. Vitale, V. Di Marzo, Identification and characterization of phytocannabinoids as novel dual PPARα/γ agonists by a computational and in vitro experimental approach., Biochim. Biophys. Acta. Gen. Subj. 1863 (2019) 586–597. doi:10.1016/j.bbagen.2019.01.002.

[12] X. Nadal, C. del Río, S. Casano, B. Palomares, C. Ferreiro-Vera, C. Navarrete, C. Sánchez-Carnerero, I. Cantarero, M.L. Bellido, S. Meyer, G. Morello, G. Appendino, E. Muñoz, Tetrahydrocannabinolic acid is a potent PPARγ agonist with neuroprotective activity, Br. J. Pharmacol. 174 (2017) 4263–4276. doi:10.1111/bph.14019.

[13] N. Malek, K. Popiolek-Barczyk, J. Mika, B. Przewlocka, K. Starowicz, Anandamide, acting via CB2 receptors, alleviates LPS-induced neuroinflammation in rat primary microglial cultures, Neural Plast. 2015 (2015) 130639. doi:10.1155/2015/130639.

[14] V.B. Lu, H.L. Puhl, S.R. Ikeda, N-Arachidonyl glycine does not activate G protein-coupled receptor 18 signaling via canonical pathways., Mol Pharmacol. 83 (2013) 267–82. doi:10.1124/mol.112.081182.

[15] G. Rajaraman, A. Simcocks, D.H. Hryciw, D.S. Hutchinson, A.J. McAinch, G protein coupled receptor 18: A potential role for endocannabinoid signaling in metabolic dysfunction, Mol. Nutr. Food Res. 60 (2015) n/a-n/a. doi:10.1002/mnfr.201500449.

[16] D. McHugh, S.S. Hu, N. Rimmerman, A. Juknat, Z. Vogel, J.M. Walker, H.B. Bradshaw, N-arachidonoyl glycine, an abundant endogenous lipid, potently drives directed cellular migration through GPR18, the putative abnormal cannabidiol receptor, BMC Neurosci. 11 (2010) 44. doi:10.1186/1471-2202-11-44.

[17] R. Nallathambi, M. Mazuz, A. Ion, G. Selvaraj, S. Weininger, M. Fridlender, A. Nasser, O. Sagee, P. Kumari, D. Nemichenizer, M. Mendelovitz, N. Firstein, O. Hanin, F. Konikoff, Y. Kapulnik, T. Naftali, H. Koltai, Anti-Inflammatory Activity in Colon Models Is Derived from Δ9-Tetrahydrocannabinolic Acid That Interacts with Additional Compounds in *Cannabis* Extracts, Cannabis Cannabinoid Res. 2 (2017) 167–182. doi:10.1089/can.2017.0027.

[18] S.K. Walsh, C.Y. Hepburn, O. Keown, A. Åstrand, A. Lindblom, E. Ryberg, S. Hjorth, S.J. Leslie, P.J. Greasley, C.L. Wainwright, Pharmacological profiling of the hemodynamic effects of cannabinoid ligands: a combined in vitro and in vivo approach, Pharmacol. Res. Perspect. 3 (2015) e00143. doi:10.1002/prp2.143.

[19] P. Morales, D.P. Hurst, P.H. Reggio, Molecular Targets of the Phytocannabinoids:

A Complex Picture, Prog. Chem. Org. Nat. Prod. 103 (2017) 103–131. doi:10.1007/978-3-319-45541-9_4.

[20] T. Hua, K. Vemuri, S.P. Nikas, R.B. Laprairie, Y. Wu, L. Qu, M. Pu, A. Korde, S. Jiang, J.H. Ho, G.W. Han, K. Ding, X. Li, H. Liu, M.A. Hanson, S. Zhao, L.M. Bohn, A. Makriyannis, R.C. Stevens, Z.J. Liu, Crystal structures of agonist-bound human cannabinoid receptor CB1, Nature. 547 (2017) 468–471. doi:10.1038/nature23272.

[21] T. Hua, K. Vemuri, M. Pu, L. Qu, G.W. Han, Y. Wu, S. Zhao, W. Shui, S. Li, A. Korde, R.B. Laprairie, E.L. Stahl, J.H. Ho, N. Zvonok, H. Zhou, I. Kufareva, B. Wu, Q. Zhao, M.A. Hanson, L.M. Bohn, A. Makriyannis, R.C. Stevens, Z.J. Liu, Crystal Structure of the Human Cannabinoid Receptor CB1, Cell. 167 (2016) 750-762.e14. doi:10.1016/j.cell.2016.10.004.

[22] Z. Shao, J. Yin, K. Chapman, M. Grzemska, L. Clark, J. Wang, D.M. Rosenbaum, High-resolution crystal structure of the human CB1 cannabinoid receptor, Nature. 540 (2016) 602–606. doi:10.1038/nature20613.

[23] X. Li, T. Hua, K. Vemuri, J.-H. Ho, Y. Wu, L. Wu, P. Popov, O. Benchama, N. Zvonok, K. Locke, L. Qu, G.W. Han, M.R. Iyer, R. Cinar, N.J. Coffey, J. Wang, M. Wu, V. Katritch, S. Zhao, G. Kunos, L.M. Bohn, A. Makriyannis, R.C. Stevens, Z.-J. Liu, Crystal Structure of the Human Cannabinoid Receptor CB2, Cell. 176 (2019) 459-467.e13. doi:10.1016/j.cell.2018.12.011.

[24] E. Martínez-Pinilla, K. Varani, I. Reyes-Resina, E. Angelats, F. Vincenzi, C. Ferreiro-Vera, J. Oyarzabal, E.I. Canela, J.L. Lanciego, X. Nadal, G. Navarro, P.A. Borea, R. Franco, Binding and signaling studies disclose a potential allosteric site for cannabidiol in cannabinoid CB2receptors, Front. Pharmacol. 8 (2017) 744. doi:10.3389/fphar.2017.00744.

[25] R.B. Laprairie, A.M. Bagher, M.E.M. Kelly, E.M. Denovan-Wright, Cannabidiol is a negative allosteric modulator of the cannabinoid CB1 receptor, Br. J. Pharmacol. 172 (2015) 4790–4805. doi:10.1111/bph.13250.

[26] M.F. Peters, C.W. Scott, Evaluating cellular impedance assays for detection of GPCR pleiotropic signaling and functional selectivity, J. Biomol. Screen. 14 (2009) 246–255. doi:10.1177/1087057108330115.

[27] A.M. Bagher, R.B. Laprairie, M.E.M. Kelly, E.M. Denovan-Wright, Methods to Quantify Cell Signaling and GPCR Receptor Ligand Bias: Characterization of Drugs that Target the Endocannabinoid Receptors in Huntington's Disease, in: Methods Mol. Biol., 2018: pp. 549–571. doi:10.1007/978-1-4939-7825-0_25.

[28] E. Khajehali, D.T. Malone, M. Glass, P.M. Sexton, A. Christopoulos, K. Leach, Biased Agonism and Biased Allosteric Modulation at the CB 1 Cannabinoid Receptors, Mol. Pharmacol. 88 (2015) 368–379.

[29] R. Franco, R. Rivas-Santisteban, I. Reyes-Resina, M. Casanovas, C. Pérez-Olives, C. Ferreiro-Vera, G. Navarro, V. Sánchez de Medina, X. Nadal, Biological potential of varinic-, minor-, and acidic phytocannabinoids, Pharmacol Res. In press (2020).

[30] H.N. Eisohly, C.E. Turner, A.M. Clark, M.A. Eisohly, Synthesis and antimicrobial activities of certain cannabichromene and cannabigerol related compounds, J. Pharm. Sci. 71 (1982) 1319–1323. doi:10.1002/jps.2600711204.

[31] C.E. Turner, M.A. Elsohly, Biological activity of cannabichromene, its homologs and isomers., J. Clin. Pharmacol. 21 (1981) 283S-291S. http://www.ncbi.nlm.nih.gov/pubmed/7298870 (accessed August 15, 2019).

[32] A.G. Granja, F. Carrillo-Salinas, A. Pagani, M. Gómez-Cañas, R. Negri, C. Navarrete, M. Mecha, L. Mestre, B.L. Fiebich, I. Cantarero, M.A. Calzado, M.L. Bellido, J. Fernandez-Ruiz, G. Appendino, C. Guaza, E. Muñoz, A cannabigerol quinone alleviates neuroinflammation in a chronic model of multiple sclerosis, J. Neuroimmune Pharmacol. 7 (2012) 1002–1016. doi:10.1007/s11481-012-9399-3.

[33] P. Weydt, S. Hong, A. Witting, T. Möller, N. Stella, M. Kliot, Cannabinol delays symptom onset in SOD1 (G93A) transgenic mice without affecting survival, Amyotroph. Lateral Scler. 6 (2005) 182–184. doi:10.1080/14660820510030149.

[34] C. Rodríguez-Cueto, I. Santos-García, L. García-Toscano, F. Espejo-Porras, Ml. Bellido, J. Fernández-Ruiz, E. Muñoz, E. de Lago, Neuroprotective effects of the cannabigerol quinone derivative VCE-003.2 in SOD1G93A transgenic mice, an experimental model of amyotrophic lateral sclerosis, Biochem. Pharmacol. 157 (2018) 217–226. doi:10.1016/j.bcp.2018.07.049.

[35] A. Smeriglio, S. V. Giofrè, E.M. Galati, M.T. Monforte, N. Cicero, V. D'Angelo, G. Grassi, C. Circosta, Inhibition of aldose reductase activity by chemotypes extracts with high content of cannabidiol or cannabigerol, Fitoterapia. 127 (2018) 101–108. doi:10.1016/j.fitote.2018.02.002.

[36] D.I. Brierley, J. Samuels, M. Duncan, B.J. Whalley, C.M. Williams, A cannabigerol-rich Cannabis sativa extract, devoid of Δ9-Tetrahydrocannabinol, elicits hyperphagia in rats, Behav. Pharmacol. 28 (2017) 280–284. doi:10.1097/FBP.0000000000000285.

[37] D.I. Brierley, J. Samuels, M. Duncan, B.J. Whalley, C.M. Williams, Cannabigerol is a novel, well-tolerated appetite stimulant in pre-satiated rats, Psychopharmacology (Berl). 233 (2016) 3603–3613. doi:10.1007/s00213-016-4397-4.

[38] G. Riedel, P. Fadda, S. McKillop-Smith, R.G. Pertwee, B. Platt, L. Robinson, Synthetic and plant-derived cannabinoid receptor antagonists show hypophagic properties in fasted and non-fasted mice, Br. J. Pharmacol. 156 (2009) 1154–1166. doi:10.1111/j.1476-5381.2008.00107.x.

[39] A. Oláh, A. Markovics, J. Szabó-Papp, P.T. Szabó, C. Stott, C.C. Zouboulis, T. Bíró,

Differential effectiveness of selected non-psychotropic phytocannabinoids on human sebocyte functions implicates their introduction in dry/seborrhoeic skin and acne treatment, Exp. Dermatol. 25 (2016) 701–707. doi:10.1111/exd.13042.

[40] J.D. Wilkinson, E.M. Williamson, Cannabinoids inhibit human keratinocyte proliferation through a non-CB1/CB2 mechanism and have a potential therapeutic value in the treatment of psoriasis, J. Dermatol. Sci. 45 (2007) 87–92. doi:10.1016/j.jdermsci.2006.10.009.

[41] A.J. Hill, C.M. Williams, B.J. Whalley, G.J. Stephens, Phytocannabinoids as novel therapeutic agents in CNS disorders, Pharmacol. Ther. 133 (2012) 79–97. doi:10.1016/j.pharmthera.2011.09.002.

[42] F. Borrelli, E. Pagano, B. Romano, S. Panzera, F. Maiello, D. Coppola, L. De Petrocellis, L. Buono, P. Orlando, A.A. Izzo, Colon carcinogenesis is inhibited by the TRPM8 antagonist cannabigerol, a Cannabis-derived non-psychotropic cannabinoid, Carcinogenesis. 35 (2014) 2787–2797. doi:10.1093/carcin/bgu205.

[43] D.G. Couch, H. Maudslay, B. Doleman, J.N. Lund, S.E. O'Sullivan, The Use of Cannabinoids in Colitis: A Systematic Review and Meta-Analysis, Inflamm. Bowel Dis. 24 (2018) 680–697. doi:10.1093/ibd/izy014.

[44] F. Borrelli, I. Fasolino, B. Romano, R. Capasso, F. Maiello, D. Coppola, P. Orlando, G. Battista, E. Pagano, V. Di Marzo, A.A. Izzo, Beneficial effect of the non-psychotropic plant cannabinoid cannabigerol on experimental inflammatory bowel disease, Biochem. Pharmacol. 85 (2013) 1306–1316. doi:10.1016/j.bcp.2013.01.017.

[45] S. Rosenthaler, B. Pöhn, C. Kolmanz, C. Nguyen Huu, C. Krewenka, A. Huber, B. Kranner, W.-D.D. Rausch, R. Moldzio, Differences in receptor binding affinity of several phytocannabinoids do not explain their effects on neural cell cultures, Neurotoxicol. Teratol. 46 (2014) 49–56. doi:10.1016/j.ntt.2014.09.003.

[46] G. Navarro, K. Varani, I. Reyes-Resina, V. Sánchez de Medina, R. Rivas-Santisteban, C. Sánchez-Carnerero Callado, F. Vincenzi, S. Casano, C. Ferreiro-Vera, E.I. Canela, P.A. Borea, X. Nadal, R. Franco, Cannabigerol Action at Cannabinoid CB1 and CB2 Receptors and at CB1-CB2 Heteroreceptor Complexes., Front. Pharmacol. 9 (2018) 632. doi:10.3389/fphar.2018.00632.

[47] E. Martinez-Pinilla, O. Rabal, I. Reyes-Resina, M. Zamarbide, G. Navarro, J.A. Sanchez-Arias, I. de Miguel, J.L. Lanciego, J. Oyarzabal, R. Franco, Two Affinity Sites of the Cannabinoid Subtype 2 Receptor Identified by a Novel Homogeneous Binding Assay., J. Pharmacol. Exp. Ther. 358 (2016) 580–587. doi:10.1124/jpet.116.234948.

[48] G. Navarro, I. Reyes-Resina, R. Rivas-Santisteban, V. Sánchez de Medina, P. Morales, S. Casano, C. Ferreiro-Vera, A. Lillo, D. Aguinaga, N. Jagerovic, X. Nadal, R. Franco, Cannabidiol skews biased agonism at cannabinoid CB1 and CB2 receptors with smaller effect in CB1-CB2 heteroreceptor complexes, Biochem.

Pharmacol. 157 (2018) 148–158. doi:10.1016/j.bcp.2018.08.046.

[49] T. Kenakin, New concepts in pharmacological efficacy at 7TM receptors: IUPHAR Review 2, Br. J. Pharmacol. 168 (2013) 554–575. doi:10.1111/j.1476-5381.2012.02223.x.

[50] T. Kenakin, Functional selectivity in GPCR modulator screening, Comb. Chem. High Throughput Screen. 11 (2008) 337–343. doi:10.2174/138620708784534824.

[51] G. Navarro, N. Franco, E. Martínez-Pinilla, R. Franco, The epigenetic cytocrin pathway to the nucleus. Epigenetic factors, epigenetic mediators, and epigenetic traits. A biochemist perspective, Front. Genet. 8:179 (2017) 1–6. doi:10.3389/fgene.2017.00179.

[52] J.L. Lanciego, P. Barroso-Chinea, A.J. Rico, L. Conte-Perales, L. Callén, E. Roda, V. Gómez-Bautista, I.P. López, C. Lluis, J.L. Labandeira-García, R. Franco, Expression of the mRNA coding the cannabinoid receptor 2 in the pallidal complex of Macaca fascicularis, J. Psychopharmacol. 25 (2011). doi:10.1177/0269881110367732.

[53] J. González-Maeso, R.L. Ang, T. Yuen, P. Chan, N. V Weisstaub, J.F. López-Giménez, M. Zhou, Y. Okawa, L.F. Callado, G. Milligan, J. a Gingrich, M. Filizola, J.J. Meana, S.C. Sealfon, Identification of a serotonin/glutamate receptor complex implicated in psychosis., Nature. 452 (2008) 93–7. doi:10.1038/nature06612.

[54] S. Ferré, R. Baler, M. Bouvier, M.G. Caron, L.A. Devi, T. Durroux, K. Fuxe, S.R. George, J.A. Javitch, M.J. Lohse, K. Mackie, G. Milligan, K.D.G. Pfleger, J.-P. Pin, N.D. Volkow, M. Waldhoer, A.S. Woods, R. Franco, Building a new conceptual framework for receptor heteromers., Nat. Chem. Biol. 5 (2009) 131–4. doi:10.1038/nchembio0309-131.

[55] R. Franco, D. Aguinaga, J. Jiménez, J. Lillo, E. Martínez-Pinilla, G. Navarro, Biased receptor functionality versus biased agonism in G-protein-coupled receptors, Biomol. Concepts. 9 (2018) 143–154. doi:10.1515/bmc-2018-0013.

[56] R. Franco, V. Casadó, A. Cortés, C. Ferrada, J. Mallol, A. Woods, C. Lluis, E.I. Canela, S. Ferré, Basic concepts in G-protein-coupled receptor homo- and heterodimerization, ScientificWorldJournal. 7 (2007). doi:10.1100/tsw.2007.197.

[57] L.C. Johansson, B. Stauch, J.D. McCorvy, G.W. Han, N. Patel, X.-P. Huang, A. Batyuk, C. Gati, S.T. Slocum, C. Li, J.M. Grandner, S. Hao, R.H.J. Olsen, A.R. Tribo, S. Zaare, L. Zhu, N.A. Zatsepin, U. Weierstall, S. Yous, R.C. Stevens, W. Liu, B.L. Roth, V. Katritch, V. Cherezov, XFEL structures of the human MT2 melatonin receptor reveal the basis of subtype selectivity., Nature. 569 (2019) 289–292. doi:10.1038/s41586-019-1144-0.

[58] B. Stauch, L.C. Johansson, J.D. McCorvy, N. Patel, G.W. Han, X.P. Huang, C. Gati, A. Batyuk, S.T. Slocum, A. Ishchenko, W. Brehm, T.A. White, N. Michaelian, C.

Madsen, L. Zhu, T.D. Grant, J.M. Grandner, A. Shiriaeva, R.H.J. Olsen, A.R. Tribo, S. Yous, R.C. Stevens, U. Weierstall, V. Katritch, B.L. Roth, W. Liu, V. Cherezov, Structural basis of ligand recognition at the human MT1 melatonin receptor, Nature. 569 (2019) 284–288. doi:10.1038/s41586-019-1141-3.

[59] G. Navarro, I. Reyes-Resina, R. Rivas-Santisteban, V. Sánchez de Medina, P. Morales, S. Casano, C. Ferreiro-Vera, A. Lillo, D. Aguinaga, N. Jagerovic, X. Nadal, R. Franco, Cannabidiol skews biased agonism at cannabinoid CB1 and CB2 receptors with smaller effect in CB1-CB2 heteroreceptor complexes, Biochem. Pharmacol. 157 (2018) 148–158. doi:10.1016/j.bcp.2018.08.046.

[60] P. Morales, P.H. Reggio, N. Jagerovic, An overview on medicinal chemistry of synthetic and natural derivatives of cannabidiol, Frontiers Media S.A., 2017. doi:10.3389/fphar.2017.00422.

[61] C. Xing, Y. Zhuang, T.H. Xu, Z. Feng, X.E. Zhou, M. Chen, L. Wang, X. Meng, Y. Xue, J. Wang, H. Liu, T.F. McGuire, G. Zhao, K. Melcher, C. Zhang, H.E. Xu, X.Q. Xie, Cryo-EM Structure of the Human Cannabinoid Receptor CB2-Gi Signaling Complex, Cell. 180 (2020) 645-654.e13. doi:10.1016/j.cell.2020.01.007.

[62] E. Martínez-Pinilla, A.I.I. Rodríguez-Pérez, G. Navarro, D. Aguinaga, E. Moreno, J.L.L. Lanciego, J.L.L. Labandeira-García, R. Franco, Dopamine D2 and angiotensin II type 1 receptors form functional heteromers in rat striatum., Biochem. Pharmacol. 96 (2015) 131–142. doi:10.1016/j.bcp.2015.05.006.

[63] G. Navarro, C. Quiroz, D. Moreno-Delgado, A. Sierakowiak, K. McDowell, E. Moreno, W. Rea, N.-S. Cai, D. Aguinaga, L.A. Howell, F. Hausch, A. Cortés, J. Mallol, V. Casadó, C. Lluís, E.I. Canela, S. Ferré, P.J. McCormick, Orexin-corticotropin-releasing factor receptor heteromers in the ventral tegmental area as targets for cocaine., J. Neurosci. 35 (2015) 6639–53. doi:10.1523/JNEUROSCI.4364-14.2015.

[64] S. Rajagopal, S. Ahn, D.H. Rominger, W. Gowen-MacDonald, C.M. Lam, S.M. Dewire, J.D. Violin, R.J. Lefkowitz, Quantifying ligand bias at seven-transmembrane receptors, Mol. Pharmacol. 80 (2011) 367–377. doi:10.1124/mol.111.072801.

[65] H.C. Cheng, The power issue: Determination of KB or Ki from IC50 - A closer look at the Cheng-Prusoff equation, the Schild plot and related power equations, J. Pharmacol. Toxicol. Methods. 46 (2001) 61–71. doi:10.1016/S1056-8719(02)00166-1.

Figure Supplementary 1

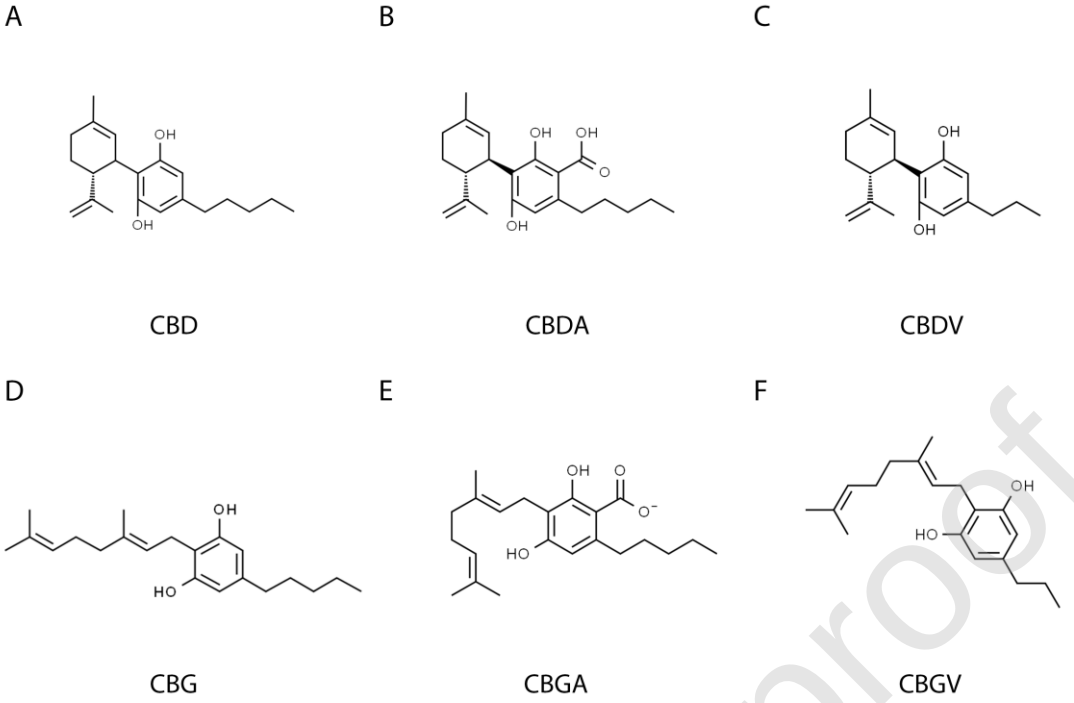

Supplementary Figure S1. Chemical structure of CBD, CBDA, CBDV, CBG, CBGA, and CBGV.

Figure Supplementary 2

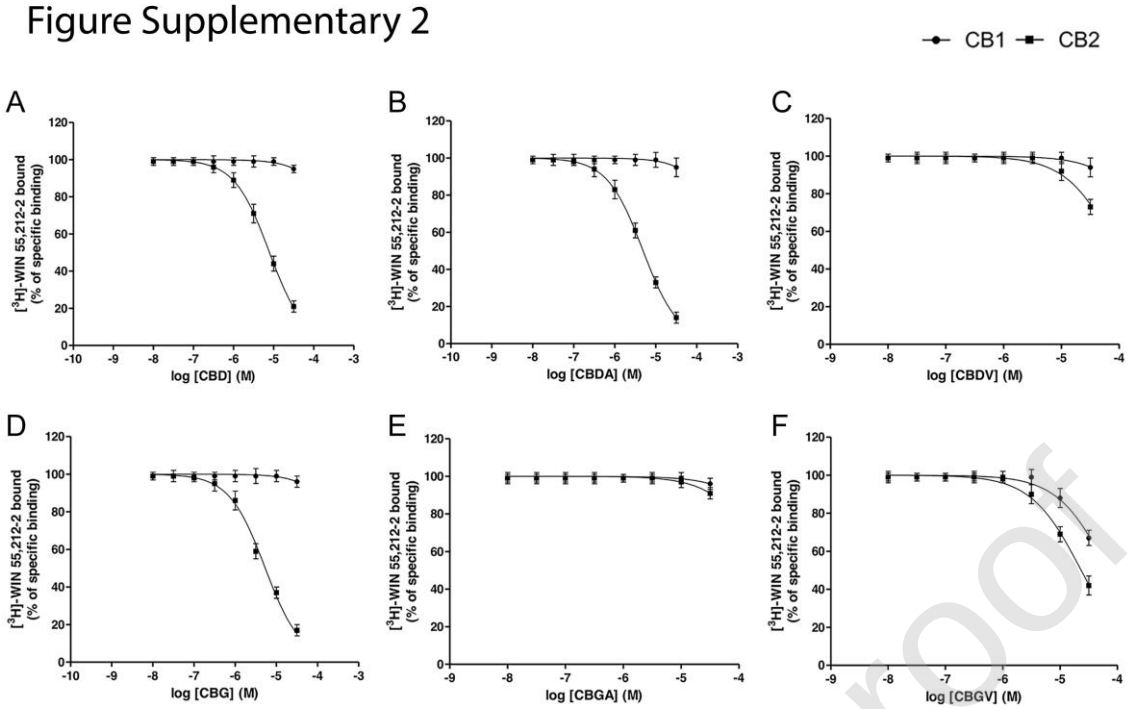

Supplementary Figure S2. Competition binding experiments of [^{3}H]-WIN 55,212-2 binding to membranes isolated from CHO cells expressing CB_1R or CB_2R

Panels A-F: Competition binding experiments were developed with the specific binding of 2 nM [^{3}H]-WIN 55,212-2 and increasing concentrations of CBD (A), CBDA (B), CBDV (C), CBG (D), CBGA (E) and CBGV (F) (0-30 μM). Data are expressed as the mean ± SEM of five independent experiments performed in duplicates.

Figure Supplementary 3

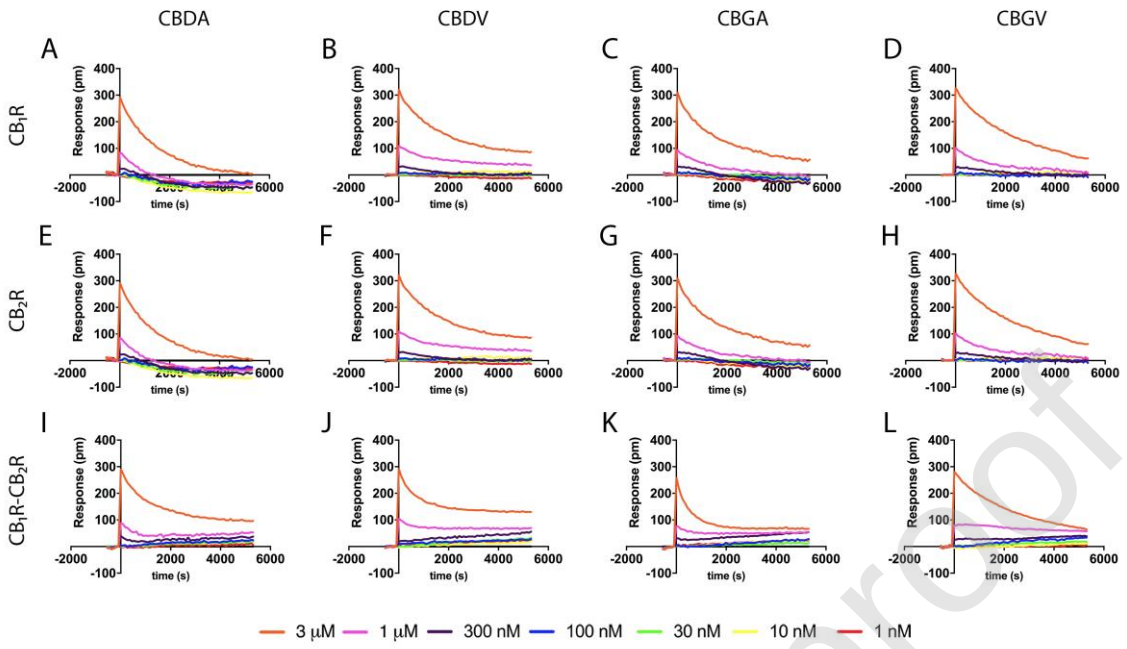

Supplementary Figure S3. CBDA, CBDV, CBGA and CBGV Dynamic Mass Redistribution characteristic signaling over CB_1 and/or CB_2 receptors

HEK-293T cells expressing CB_1R (0.75 μg cDNA) (A-D), CB_2R (1 μg cDNA) (E-H) or CB_1R (0.75 μg cDNA) and CB_2R (1 μg cDNA) (I-L) were treated with CBDA (A, E, I), CBDV (B, F, J), CBGA (C, G, K) or CBGV (D, H, L). DMR dose–response curves (1 nM to 3 μM range) were analyzed and represented as lineal signals during a period of 5,000 seconds. Data from representative experiments are shown.